CHAPTER 3

Probing the folded and unfolded states of OmpA tryptophan mutants using steady-state and time-resolved tryptophan fluorescence

Adapted from Kim J.E., Arjara G., Richards J.H., Gray H.B, and Winkler J.R. *J.Phys.Chem.B* 2006, 110, 17656-17662.

Acknowledgement: Experiments were done in collaboration with Dr. Judy E. Kim.

3.1 INTRODUCTION

Depending on the environment, OmpA can exist in five different conformations: unfolded in aqueous urea, aggregated in water, folded in detergent micelles, folded in lipid bilayers, and partially folded/adsorbed to the lipid bilayer surface (Surrey & Jahnig, 1992; Surrey & Jahnig, 1995).

Previous studies reported that unfolded OmpA in 8 M aqueous urea exhibited a random structure in the circular dichroism (CD) spectrum and relative weak and polar emission maximum at ~350 nm for the tryptophans. Dilution of urea with phosphate buffer produces a CD spectrum indicating that the aggregated state is a mixture of α-helical, β-sheet, and random-coil structure. The Trp fluorescence intensity remains relatively weak but the emission maximum is slightly blue-shifted to 343 nm. When OmpA is diluted with a solution of DMPC vesicles, the CD spectrum shows a β-sheet signal and the Trp fluorescence is high with a hydrophobic emission maximum at 325nm. Similarly, OmpA folded in OG micelles exhibit β-sheet signal and blue-shifted emission maximum (Surrey & Jahnig, 1992).

For OmpA to refold into lipid bilayers, the lipid vesicles must be above their gel-liquid transition temperature and the bilayer generally must be highly curved as in SUVs. Folding has been observed into LUVs under small membrane thickness conditions (Kleinschmidt & Tamm, 2002). The large amounts of defects in SUVs due to suboptimal packing of lipids allow the hydrophobic interior to interact with OmpA. Depending on the carbon chain length of the lipid, LUVs will generally not permit OmpA to adsorb or insert in the vesicles unless defects such as those introduced by detergents are present (Surrey & Jahnig, 1992). Early reports have shown that OmpA in DMPC vesicles has

~50-60 % β-sheet structure and that the tryptophan residues are in a strongly hydrophobic environment (Vogel & Jahnig, 1986; Dornmair et al., 1990; Rodionova et al., 1995). Trypsin digestion experiments of folded OmpA in DMPC vesicles revealed that ~99 % of OmpA was oriented with their peripheral part outside the vesicles (Figure 2.3).

When OmpA was allowed to interact with DMPC vesicles at 15 ^{o}C, below the lipid phase transition temperature of 23 ^{o}C, CD spectra revealed similar β-sheet content and steady state fluorescence revealed blue-shifted Trp emission maximum similar to the spectrum of protein folded in DMPC at 30 ^{o}C. However, gel-shift assays showed the protein migrated at 35kDa and was susceptible to complete digestion by trypsin. In this adsorbed state, FTIR revealed about 45 % β-sheet content (Rodionova et al., 1995). As the urea concentration was increased, the adsorbed protein became unfolded. When the temperature was slowly raised from 15 ^{o}C to 30 ^{o}C, OmpA refolded and inserted as if refolding took place at 30 ^{o}C (Surrey & Jahnig, 1992).

The transmembrane region was previously studied by trypsin digestion of the cell membranes, followed by OmpA purification. Similar CD and fluorescence signals were observed for this transmembrane truncated-OmpA. In 8 M urea, both truncated-OmpA and full-length OmpA showed no secondary structure. In 4 M urea, the C terminal domain showed some secondary structure for the full-length OmpA but not for the truncated-OmpA. Glu-C endoproteinase was used to remove the remainder of the periplasmic region undigested by trypsin, producing a 21 kDa molecular mass. This revealed that the truncated-OmpA refolded unidirectionally into vesicles. These studies have shown that the C-terminal tail is not required for oriented insertion of OmpA and

that the orientation of OmpA within the membrane appears to be related to the mechanism by which the protein inserts.

Fully folded OmpA *in vitro* has the same properties as native OmpA from spectroscopic studies such as CD, FTIR, Raman and fluorescence, and from biochemical techniques including proteolysis, gel-shift assays (Dornmair 1990, Surrey 1992, 1995, Kleinschmidt 1999, Rodionova 1995, Vogel and Jahnig 1986). Refolded and native OmpA were both shown to form ion channels in planar lipid bilayers (Arora et al., 2000).

The transmembrane domain structure of OmpA has been solved by X-ray crystallography and NMR using protein folded in detergents (Pautsch & Schulz, 2000; Arora et al., 2001). Aromatic amino acids were found to be at the bilayer-water interface, consistent with the position of these residues in other membrane protein structures (Schiffer et al., 1992; Cowan & Rosenbusch, 1994). We do not currently know the structure of the full-length OmpA and whether the C-terminus affects the transmembrane structure. One of our aims was to use fluorescence spectroscopy to compare the Trp environments of OmpA in detergent micelles and lipid vesicles (Figure 3.1). The two different environments could affect the overall structure in that the ordered packing in lipid bilayers may expose OmpA dynamics to different motional constraints than that from the more fluid micelles. There is greater restriction in movement for phospholipids than in detergents, especially in the polar head groups.

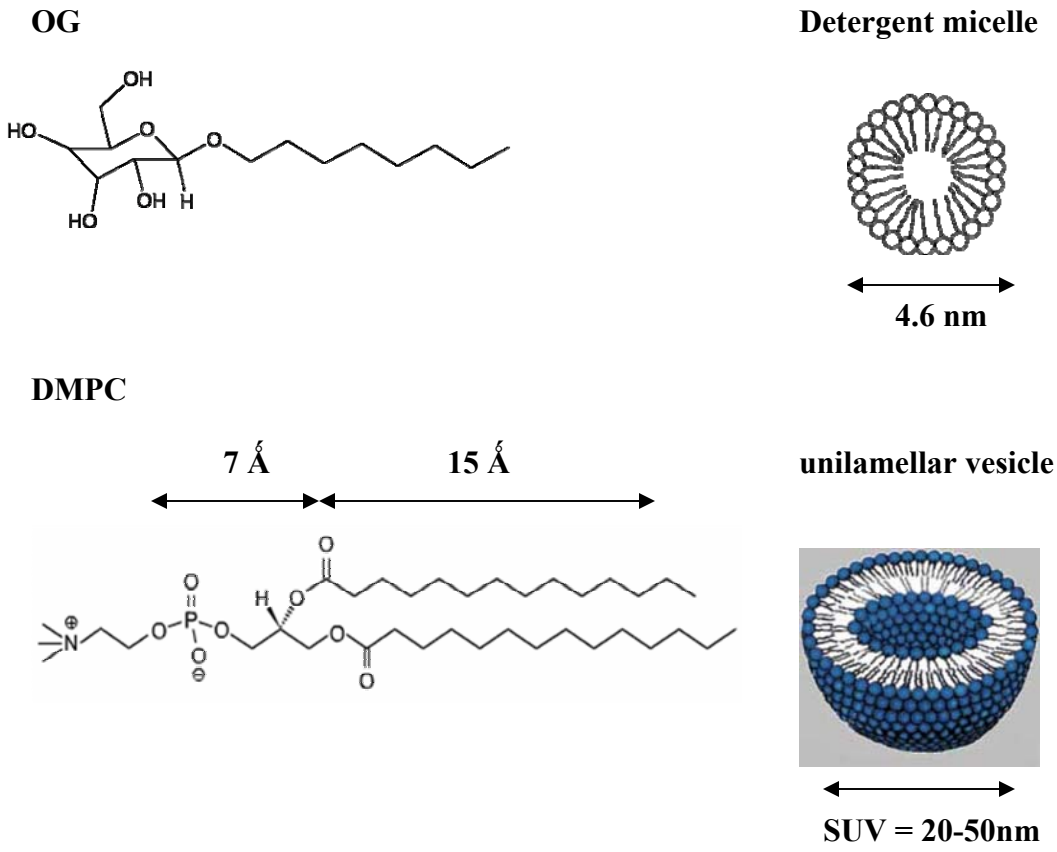

Figure 3.1. Structures of OG detergent and DMPC phospholipid. Illustrations of a detergent micelle and unilamellar vesicles are shown, along with approximate sizes.

3.2 EXPERIMENTALS

Steady-state absorption spectra (UV-visible spectroscopy)

For all samples used, UV-visible absorption spectra were obtained on a Hewlett-Packard 8453 diode-array spectrophotometer. Background spectra of either urea-only, phosphate buffer-only, OG micelles-only, or DMPC vesicles-only were recorded and subtracted from protein absorption spectra. Estimation of protein concentrations for wild-type OmpA, full-length mutants, and truncated mutants were calculated using ε_{280}=54,390 $M^{-1}cm^{-1}$, ε_{280}=32,330 $M^{-1}cm^{-1}$, ε_{280}=26,020 $M^{-1}cm^{-1}$, respectively.

Circular dichroism spectroscopy

A 1 mm fused silica cuvette with ~6 μM protein was used to obtain CD spectra, recorded on an Aviv 62ADS spectropolarimeter (Aviv Associates, Lakewood, NJ). Room temperature measurements were taken on samples in urea and OG micelles while 15 ^{o}C and 30 ^{o}C measurements were recorded for samples in DMPC vesicles and phosphate buffer. CD scans were recorded from either 190 or 200 nm to 260 nm at 1 nm/step with an integration time of 3 sec and a bandwidth of 1.5 nm. Background spectra of either 8 M urea, phosphate buffer, OG micelles, or DMPC vesicles were recorded and subtracted from protein spectra. Spectra values were read as mdeg and were converted to molar ellipticity (Θ; units of deg cm^2 $dmol^{-1}$) using Θ = mdeg/10/cuvette pathlength (cm)/protein residues/protein molarity.

Steady-state fluorescence spectroscopy

Steady-state tryptophan fluorescence spectra and anisotropy were recorded on a Jobin Yvon/SPEX Fluorolog spectrofluorometer (Model FL3-11) equipped with a Hamamatsu R928 PMT. Protein samples of ~3 μM in 1 cm quartz cuvettes were excited

with photons of λ = 290 nm (2nm bandpass) and emission was recorded from λ = 300-500nm (2 nm and 4 nm bandpass for fluorescence and anisotropy, respectively) with 2 nm/step and 0.5 sec integration at 30 ^{o}C and 15 ^{o}C. Similar to measurements from CD and UV-visible spectroscopy, background spectra were recorded and subtracted in the analysis.

Steady-state anisotropy

For steady-state anisotropy, polarization filters were placed before and after the sample. For each protein sample, four spectra were measured, I_{VV}, I_{VH}, I_{HH}, and I_{HV}, where the first (V = vertical) and second subscripts (H = horizontal) correspond to the excitation and emission polarization beams, respectively. The following equation was used to determine steady-sate anisotropy, r_{ss}, for each protein sample (Lakowicz, 1999):

$$r_{ss} = \frac{I_{VV} - GI_{VH}}{I_{VV} + 2GI_{VH}}, \text{ where } G = I_{HV}/I_{HH}.$$

NATA (*N*-acetyltryptophanamide; Sigma-Aldrich) was used for control samples to determine the G-factor, which is the sensitivity of the instrument for vertically and horizontally polarized light.

Time-resolved fluorescence spectroscopy

Protein samples consisted of 1.2 mL of ~3 μM protein in a 1 cm path-length quartz cuvette containing a small magnetic stir bar and sealed with a rubber septum. Prior to exited-state lifetime and anisotropy decay measurements, protein samples in DMPC vesicles were kept in a 35 ^{o}C oven for at least 3 hours. Immediately before measurements, samples were deoxygenated ~10 min with 5-6 cycles vacuum pumping and argon-filling in a 30 ^{o}C water bath with stirring. A temperature-controlled cuvette holder was used to maintain sample temperature at 30 ^{o}C during measurements.

Figure 3.2 illustrates the laser setup that was used to collect time-resolved fluorescence. A femtosecond Titanium:Sapphire regenerative amplifier (Spectra-Physics) was used to excite samples at a 1 kHz repetition rate with 290 nm (292 nm for the experiments found in Chapters 5 and 6) pulses from the third harmonic. The time resolution of the laser is determined by the full width at half maximum (FWHM) of the instrument response function, which is ~300 ps. Excitation power at the sample was ~550-650 μW and a 355 ± 5 nm (or 325 ± 5 nm) filter was used to select for tryptophan emission. In later experiments found in Chapters 5 and 6, an additional UG11 glass filter was used that allows passage of only ultraviolet light below 400 nm. Excited-state decay kinetics were recorded using an optical fiber connected to a picosecond streak camera (Hamamatsu C5680) with 9-15 min (or 4-6 min in Chapters 5 and 6) integration times in photon-counting mode. Measurements were recorded under magic angle polarization conditions (O'Connor & Phillips, 1984) and emission was detected at 90 ^{o} to the excitation beam. Minimal photobleaching (<10 %) was confirmed by recording UV-visible absorption spectra before and after laser measurements. Data sets for all mutants under the various conditions (unfolded in urea, folded in OG and DMPC) were obtained on the same day to ensure that lifetimes could be compared to one another. The lifetime of NATA was always measured at the start of the experiments to ensure that data sets from different days could be compared.

Anisotropy decay kinetics

The laser configuration and experimental setup for anisotropy decay kinetics is the same as in excited-state decay measurements except that the excitation beam was vertically or horizontally polarized and the emission was selected using polarizers

oriented vertically or horizontally. Samples were excited with 900 μW power. NATA (*N*-acetyl-L-tryptophanamide) was used to determine the G value.

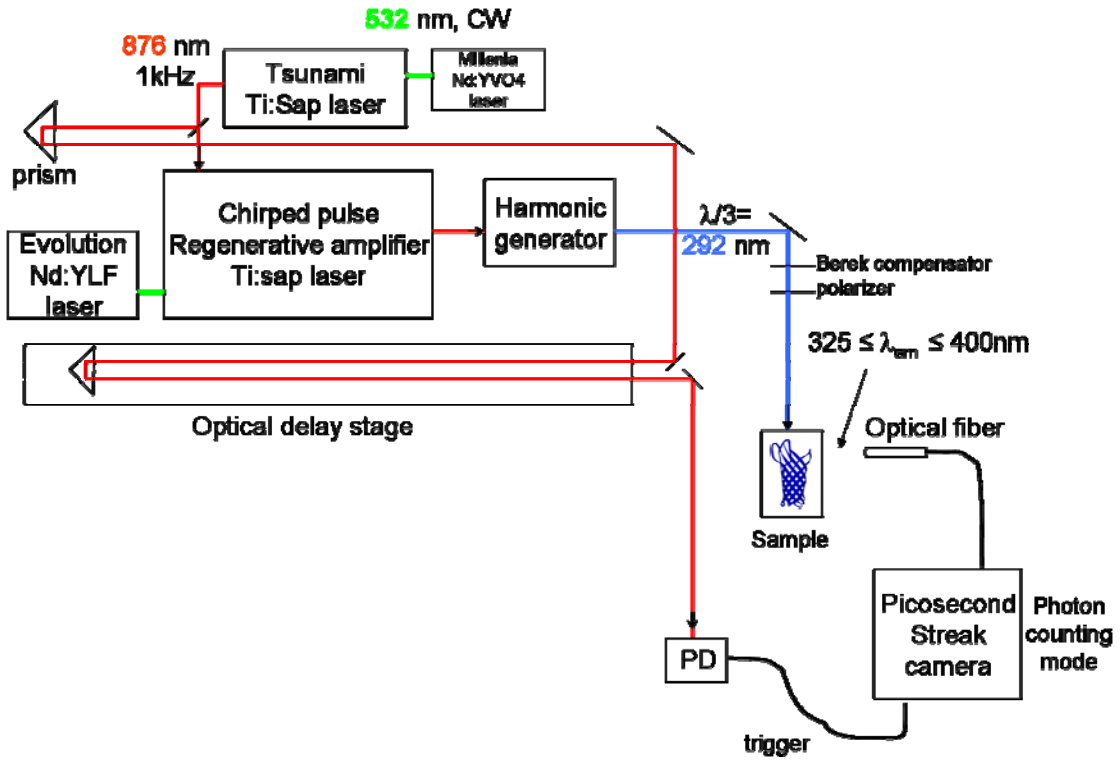

Figure 3.2. Schematic of the setup for time-resolved measurements using the femtosecond Titanium:sapphire (Ti:Sap) laser and the picosecond streak camera. Not all optical parts are illustrated. Figure not drawn to scale. Abbrevation PD = photodiode.

3.3 RESULTS AND DISCUSSION

Circular dichroism spectra

Far UV CD spectra (190-250 nm) provides information on secondary structure of proteins. Plane polarized light, composed of left and right circularly polarized light, is passed through the sample solution. In a solution with optically active molecules, left and right polarized light will be absorbed in different amounts, thus providing different signals for random coils, α-helices and β-sheets. CD is a relatively fast way to qualitatively measure changes in conformation and predict the amount of secondary structure in a protein. For instance, CD can be used to study how the molecule's secondary structure changes as a function of temperature or the concentration of denaturants. Therefore, it can provide thermodynamic information about the molecule that cannot be easily obtained with other methods (Beychok, 1966; Greenfield, 1996).

The CD spectra of wild-type OmpA and its tryptophan mutants report on the secondary structure of the proteins in different environments (Figures 3.3, 3.4). In 8 M urea, the protein is unfolded as indicated by the absence of secondary structure in the CD (Figure 3.3). Under folding conditions in micelles and vesicles, the proteins exhibit the characteristic β-sheet signal centered at 212 nm and 216 nm for the full-length and truncated proteins, respectively (Figure 3.4). The CD spectra for the mutants in micelles and vesicles are similar. Wild-type OmpA and full-length mutants show similar CD signal, suggesting that mutating 4 out of 5 native Trps to phenylanines (Phe) did not disturb the general β-barrel. This result is consistent with earlier reports of similar phage-binding activity for full-length single Trp mutants and wt-OmpA. It was concluded that the mutations did not alter the topology and extracellular surface structure of OmpA

(Kleinschmidt et al., 1999). The CD signal is slightly broad at the far UV end of the spectra, possibly due to either additional secondary structure that we do not know of yet in the C-terminus or higher urea concentrations in the final mixture that affected spectra below ~202 nm. Compared to the truncated proteins, it was difficult to concentrate full-length OmpA so a larger amount of full-length stock solution was used to obtain ~6 μM protein in DMPC vesicles.

For the truncated tryptophan variants, where the C-terminal tail was removed, a slightly red-shifted CD signal and a decrease in molar ellipticity are observed. Compared to full-length protein, the spectra for truncated mutants has a signal that appears more consistent with pure β-sheet structure, indicating that the transmembrane region is composed of β-sheets. This is in agreement with information revealed by the two structures of OmpA (Pautsch & Schulz, 1998; Arora et al., 2001). The loss in CD signal suggests that the C-terminus may have some β-sheet or even some small amount of α-helical secondary structure. Other laboratories observed that a small population of OmpA forms a large pore with a structure resembling porin's 16-stranded β-barrel where the C-terminus is inserted into the transmembrane region (Sugawara & Nikaido, 1994; Zakharian & Reusch, 2005). Our CD data is consistent with this observation in that increased secondary structure is observed with the C-terminus. If this large OmpA barrel exists in large populations, it does not significantly alter the local Trp environment as evidenced by only minor differences in fluorescence properties of truncated and full-length proteins, which are described in the following subsections.

The CD spectra for mutants in buffer differ noticeably from spectra in urea (Figure 3.3). The characteristic β-sheet signal when OmpA is placed in buffer is not

observed but there may be some secondary structure, such as a mixture of α, β, and random structure. This is consistent with previous CD spectra of OmpA in buffer (Surrey & Jahnig, 1992; Surrey & Jahnig, 1995) (Surrey et al., 1996), which reported that partial structure with some β-sheet is observed within the mixing deadtime of 1 s (Surrey & Jahnig, 1995). Indeed, tryptophan fluorescence of mutants in water shows a slight blue-shift compared to spectra in urea (Figure 12). Our CD spectra of OmpA in buffer are not as smooth as those in the literature, probably because reported data were smoothed or due to aggregation of proteins in our cuvette, since some particulates were observed on the cuvette and spectra were not taken immediately after dilution.

The CD spectra for mutants at 15 ^{o}C are similar to those at 30 ^{o}C, indicating that this adsorbed state contains a significant amount of secondary structure. When the spectra from the two temperatures are overlayed, we see that the truncated proteins have similar signals however the full-length mutants show some differences. Full-length spectra at 15 ^{o}C are slightly broader around 220 nm suggesting that maybe some α-helical structures are present, possibly due to the C-terminal domain.

Steady-state fluorescence

Compared to the other fluorescent amino acids, the use of Trp as an intrinsic probe of proteins is advantageous due to its higher quantum yield, longer excited-state lifetime, and sensitivity of its fluorescence to the environment (Lakowicz, 1999). NATA is a closely related structural analog of Trp, and therefore is commonly used as a control for studying Trp in proteins. Steady-state fluorescence spectra for NATA in urea, buffer, OG micelles, and DMPC vesicles exhibit the same λ_{max} and the larger Stokes shift (72nm, λ_{abs} 280 nm, λ_{em} 352 nm) when compared to protein spectra (Figure 3.6). For

NATA and other non-hydrogen bonded systems, the Stokes shift is correlated with solvent refractive indices and dielectric properties (Szabo & Rayner, 1980). In both micelles and vesicles, the observed shifts for NATA are consistent with a polar environment for the indole side chain, indicating NATA is not located inside a micelle or vesicle bilayer.

Relative to NATA, Trp emission in the unfolded state is slightly blue-shifted with a λ_{max} at 346 nm (Figure 3.7), indicating some possible residual structure that does not appear in the CD signal (Figure 3.3, top). The Stokes shift decreases to 38-48 nm upon folding the proteins in micelles (Figure 3.8) or vesicles (Figure 3.9) with emission maxima ranging from 318 to 328nm and an increase fluorescence quantum yield. The blue shift of the emission spectra and increase in quantum yield are due to the increased hydrophobic environment of the Trps in the folded state. There are only slight differences in the spectra between full-length and truncated proteins, indicating that the Trp microenvironment, and thus the OmpA transmembrane structure, may only be minimally affected by the presence of the periplasmic C-terminal tail.

The emission maxima for different Trp location varies slightly from one another. For example, W7 usually results in the most blue-shifted spectra with λ_{max} of 322 nm in micelles and 318 nm in vesicles (Table 3.1). This observation was also previously reported with W7 (Kleinschmidt et al., 1999), suggesting that W7 may be in the most hydrophobic environment compared to the other Trps. Among the Trp residues, W7 fluorescence is the most quenched by brominated lipids, suggesting that it is closest to the hydrocarbon center (see Chapter 4) and supports the evidence that W7 is in the most hydrophobic environment.

Fluorescence spectra at 15 ^{o}C for both full-length and truncated mutants indicate that the Trp residues are placed in a hydrophobic environment, similar to that of 30 ^{o}C (Figures 3.10, 3.11). This supports results from CD spectra taken at 15 ^{o}C where we observed secondary structure formation for the mutants. Therefore at 15 ^{o}C, the protein is in an ordered state that has β-sheet structure and hydrophobic Trp environments. However, it is uncertain whether this has similar structure to the 30 ^{o}C folded species. It has been speculated that the 15 ^{o}C adsorbed species is a folding intermediate since raising the temperature above 23 ^{o}C allows the protein to fold into the DMPC vesicles (Rodionova et al., 1995). Whether this is a true intermediate in the folding pathway is further discussed in Chapter 6 using fluorescence energy transfer kinetics.

The first step in OmpA folding is the transition from the unfolded state in 8 M aqeous urea to the partially folded state in water (phosphate buffer). Similar to spectra in urea, steady-state fluorescence of the mutants in phosphate buffer shows slight blue-shifting of the emission maxima, ~346 nm, compared to NATA (Figure 3.12). This suggests that the Trp are in a slightly more hydrophobic environment in both urea and phosphate buffer. Despite the similarities of the Trp environment in urea and water, the CD spectra indicate that the two species have different secondary structures.

Time-resolved fluorescence

Trp absorbs and emits near the ultraviolet range. The indole moiety of tryptophan contains two low-lying singlet excited states ($^{1}L_{a}$ and $^{1}L_{b}$) twith similar energies. The $^{1}L_{a}$ state fluorescence is red-shifted in polar solvents while fluorescence from the $^{1}L_{b}$ state is insensitive to the environment (Lami & Glasser, 1986). Interconverions between these two overlapping electronic transitions contributes to multiexponential decays observed

for Trp. Equilibrium mixture and interconversion of Trp conformers also result in multiexponential decays (Szabo & Rayner, 1980; Beechem & Brand, 1985).

In proteins, excited-state electron and proton-transfer mechanisms by residues, including tyrosines and glutamine, quench the singlet excited-state of Trp (Chen & Barkley, 1998). Excited-state Trp decays are also affected by local solvent polarity and refractive indices (Toptygin et al., 2002). Therefore, any observed variations in lifetimes for folded proteins in micelles and vesicles reflect the different microenvironments for an individual tryptophan under the different conditions. We used time-resolved fluorescence to investigate the local environment around the Trp residues in the unfolded (urea) and folded state (micelles and vesicles).

NATA excited-state decay kinetics in urea, buffer, micelles, and vesicles are fitted to either mono-, bi-, or triexponential decays (Figure 3.13, Table 3.2). These multiexponential decays are also expected for Trp fluorescence kinetics. However, Trp fluorescence decays are different from the decays of NATA in both denaturing (Figure 3.14) and folding (Figures 3.15, 3.16) conditions. In 8M urea, biexponential fits and sometimes triexponential fits of the decay kinetics reveal faster lifetime decays for unfolded protein compared to the decays of free NATA decays (Table 3.3). Also, the decay kinetics reveal that when unfolded, the microenvironments of the Trps are not identical indicating some structural retention. Previous research has observed residual structure in other proteins in the denatured states such as cytochrome *c* and indicates that unfolded proteins may not behave like random coils (Pletneva et al., 2005). Full-length and truncated proteins show similar tryptohan fluorescence decays, indicating that the C-terminal tail does not affect this possible deviation from a random coil.

When folded in micelles and vesicles, Trp excited-state lifetimes increase (Figures 3.15, 3.16, Tables 3.4, 3.5). At first glance, lifetimes in vesicles appear shorter than those in micelles (Figure 3.17, Table 3.7) but these differences may be due to the different solvent environments since NATA also exhibits different lifetimes in micelles and vesicles. As described, the differences in lifetimes of Trp reflect the different microenvironments. Trp lifetimes in OG and DMPC are slightly different, but do not suggest that the OmpA structures are different in the two environments. High resolution structures of OmpA, solved by NMR and X-ray diffraction, have been collected from protein folded in micelles.

These lifetimes are consistent with a previous report on Trp lifetimes in wild-type OmpA denatured in guanidine hydrochloride and folded in vesicles (Doring et al., 1995). Furthermore, the absence of the C-terminal tail does not drastically affect the lifetimes of the Trp and therefore their microenvironment is only minimally affected (Tables 3.3, 3.4, 3.5). These results are consistent with steady-state fluorescence data where the emission maxima are similar between full-length and truncated Trp mutants.

Lifetimes at 15 ^{o}C (Figure 3.18) cannot be directly compared to those at 30 ^{o}C because lifetimes become longer at lower temperatures since processes are slower at low temperatures. Biexponential fits of truncated and full-length lifetimes are mostly similar to one another, indicating that the C-terminus does not affect the Trp microenvironment even in the adsorbed state (Table 3.6). Table 3.7 summarizes the weighted lifetimes of the Trp mutants in the three different environments.

Steady-state fluorescence anisotropy

The Trp microenvironment was further investigated via fluorescence anisotropy measurements, which should reveal the extent of Trp structural rigidity within the unfolded and folded states. The spectra are shown in Figure 3.19, 3.20, 3.21 as reference material but are slightly misleading due to noise from vesicle scattering and thus, seem to suggest that the anisotropy varies with emission wavelength. In general, however, the steady-state anisotropy exhibits little variation with the emission wavelength (Lakowicz, 1999). Therefore, the anisotropy values were averaged over all emission wavelengths and the results are listed in Table 3.8. When the proteins are unfolded in urea, the anisotropy is about zero. Upon folding in micelles, the anisotropy increases to ~ 0.1, similar to a previous report of tryptophan anisotropy in cold propylene glycol solution (Valeur & Weber, 1977). Differences between full-length and truncated proteins in urea and micelles are minimal. When the proteins are folded in DMPC vesicles, the anisotropies of the full-length mutants further increase to ~ 0.13 and exhibit slight variations among the Trp positions. The anisotropies of the truncated mutants increase to ~ 0.2 in vesicles.

The listed anisotropy values represent upper limits due to strong vesicle scattering, dependent on polarization. Spectra of vesicle-only samples showed strong scattering in the far-UV region. These background spectra were subtracted from polarized OmpA spectra; therefore variations in the shape of vesicle-only spectra affected the corrected polarized protein spectra. The higher anisotropy values for truncated mutants are not realistic, however, because the steady-state anisotropy cannot be higher than the anisotropy at time zero, which is 0.17 for 290 nm excitation (Ruggiero et al.,

1990). This higher than realistic value of the steady-state anisotropy may be due to greater polarization-dependent scattering from vesicles due to the removal of the periplasmic domain possibly facilitating vesicle fusion. Truncated protein samples, especially W7t, were sometimes observed to be slightly cloudy supporting this theory.

Time-resolved fluorescence anisotropy

Time-resolved fluorescence anisotropy studies of proteins and peptides have the potential of providing direct insight to structural fluctuations that take place during the excited state lifetime of a protein fluorophore. This method has been widely used to study segmental mobility of proteins including myosin and immunoglobulins with external fluorescent probes (Yguerabi.J et al., 1970; Mendelso.Ra et al., 1973; Lovejoy et al., 1977), and to investigate structure and dynamics in proteins such as human serum albumin and azurin (Munro et al., 1979; Beechem & Brand, 1985). An isotropic sample (independent of direction) is preferentially excited by vertically polarized light. Randomization of the orientation of this ensemble of excited molecules causes depolarization and is achieved by rotational Brownian motion. The extent of depolarization is affected by the fluorophore's flexibility relative to the macromolecule and by the size, shape, and internal motions of the macromolecule. The depolarization can be measured by collecting the vertical and horizontal emission with respect to time (Lakowicz, 1999). To study the relative mobilities of the Trp residues in OmpA, we used time-resolved emission anisotropy in the three different Trp environments.

The overall steady-state fluorescence anisotropy is a contribution of various dynamic events taking place on a wide range of timescales, such as local tryptophan motions (~subnanoseconds), polypeptide segmental flexibility (few ns), and global

orientational motion of the entire vesicle or of the whole protein (tens to hundreds of ns). Therefore, direct information of structural dynamics during the excited-state lifetime of tryptophan can be obtained from fluorescence anisotropy decay measurements. Emission anisotropy decays are shown for mutants in urea, micelles, and vesicles in a 50 ns (Figures 3.22, 3.23, 3.24) and a 5 ns time window (Figure 3.26). Although the anisotropy data are noisy due to vesicle scattering, some information can be extracted from the results. Correlation times from biexponential fits of the Trp anisotropy decays in the various environments are shown in Table 3.9.

The motions of a single residue are less than 100 ps, which is not detectable by our instrument's temporal response (~ 300 ps). Therefore, the anisotropy decays shown reflect the dynamics of the entire protein and/or its subsections. Anisotropy decays of the Trp residues in urea reveal fast (~0.9 ns) and slow (~6 ns) correlation times from the biexponential fits. These decays are due to segmental rotational correction times of the protein subsections in the unfolded state. All Trp mutants show that the anisotropy decays to zero within the excited-state lifetime of Trp. Despite variations of local Trp environment (Tables 3.1, 3.10), similar correlation times among the mutants suggest that the subsections near the Trp have similar dynamics. If there is any residual structure in the unfolded protein it does not change the local correlation time. This observation is reasonable since factors affecting Trp lifetimes are not the same as those affecting anisotropy decay kinetics.

When folded in OG micelles, the anisotropy decays of the proteins increase to ~2 ns and 11 ns, reflecting a more hindered environment for the Trp in the folded state. Compared to those in urea, the anisotropies do not decay to zero within the time of the

singlet excited-state. This is interpreted as the slower tumbling of the protein subsections or of the whole detergent micelle.

Evaluation of time-resolved fluorescence depolarization kinetics should include the experimental value of the anisotropy at time zero (r_o). This value is the intrinsic anisotropy of the fluorophore and is a function of the relative orientations of the absorption and emission transition dipole moments. If a fluorophore has parallel absorption and emission transition dipoles, the value for r_o is theoretically 0.4 (Ruggiero et al., 1990). Therefore if r_o values less than 0.4 are observed, there is probably some kind of relaxation process occurring on a timescale shorter than the instrument response. It should be noted that the r_o value of Trp varies with the excitation wavelength. With excitation at 290 nm, the published r_o value for tryptophan is 0.17 (Ruggiero et al., 1990). Our r_o values are consistent with these previous studies. In addition, all the mutants in the unfolded state have similar r_o values. In OG micelles, r_o values are similar among the mutants except for W7. Upon folding in DMPC vesicles, mutants exhibit fast and slow correlation times of 2 ns and 26 ns as well as increased variations in r_o values. The increase in the slow correlation time reflects the larger size of the vesicles and the more viscous environment of the lipids. The differences in r_o values at the different positions when folded in vesicles suggest various degrees of Trp residue motions that we cannot detect on the experimental timescale. The anisotropies also take longer to decay to zero within the time of the Trp excited state.

According to the steady-state fluorescence, W7 is the most hydrophobic of the five Trp and accordingly, W7 is expected to interact with the very fluid hydrocarbon core of the lipid vesicles the most (Brown et al., 1979). Indeed, we observe that W7 is the

least hindered Trp, in both OG micelles and DMPC vesicles. Results from the 5 ns timescale experiments confirm that W7 has the lowest anisotropy (Figure 3.26). There have been studies that measured anisotropy decays of Trp residues along a transmembrane polypeptide as well as along a peptide laterally associated with lipids (Vogel et al., 1988; Clayton & Sawyer, 2000). Compared to Trp residues in the middle of the peptide, Trp near the ends of the peptide are more flexible. This may be the case for W7 since it is located at the beginning of the protein.

W7 may also be more dynamic compared to other Trp because this β-sheet strand may interact directly with the C-terminal tail for formation of the barrel structure. When anisotropies of truncated mutants are compared, W7t also has the lowest r_o of the Trp residues. Despite elimination of the C-terminal tail, this β-sheet strand is still more dynamic than the other Trps. W15 is the next least hindered Trp residue and also resides on the same β-strand as W7.

Comparison of the anisotropies among the full-length and truncated Trps in DMPC vesicles show similar anisotropies for most mutants (Figure 3.25). W102t shows a higher r_o value and slower correlation time than the full-length mutant W102, probably due to higher vesicle scattering from the truncated sample.

We can still learn something about the lipid bilayer environment from these experiments. Despite the DMPC vesicles being above their gel-liquid transition temperature, the environment of the bilayer is still more viscous than that of OG micelles, disallowing the same freedom of movement as micelles. Furthermore, the larger vesicle sizes (~20-50 nm diameter) will tumble more slowly than the smaller micelles (~5 nm diameter). The Trp are more hindered in this environment. More detailed information

such as exact correlation times could not be obtained due to the low signal to noise ratio in the data. This issue might be resolved if Trp was excited at 300 nm rather than 290 nm (Ruggiero et al., 1990). This will allow higher r_o values to be obtained. Anisotropy at low temperatures may also help further characterize the adsorbed state.

3.4 CONCLUSIONS

Time-resolved fluorescence and anisotropy measurements are sensitive techniques for probing the folded state of membrane proteins such as OmpA. These techniques provide a complement to steady-state measurements and further our physical understanding of membrane protein folding. CD and steady-state fluorescence show that both protein species at 15 ^{o}C and 30 ^{o}C have β-sheet signal and blue-shifted emission maxima. These two species are further described in Chapters 5 and 6. Results also suggest that the transmembrane structure of OmpA is not affected significantly by the C-terminal domain. Anisotropy revealed that W7 is the least hindered residue, possibly due to its closer location to the fluid hydrocarbon core or due to the dynamics of the C-terminal domain. These results lay the foundation for further lifetime measurements of membrane protein folding and for advanced spectroscopic investigations such as fluorescence energy transfer kinetics, which is discussed in Chapter 6.

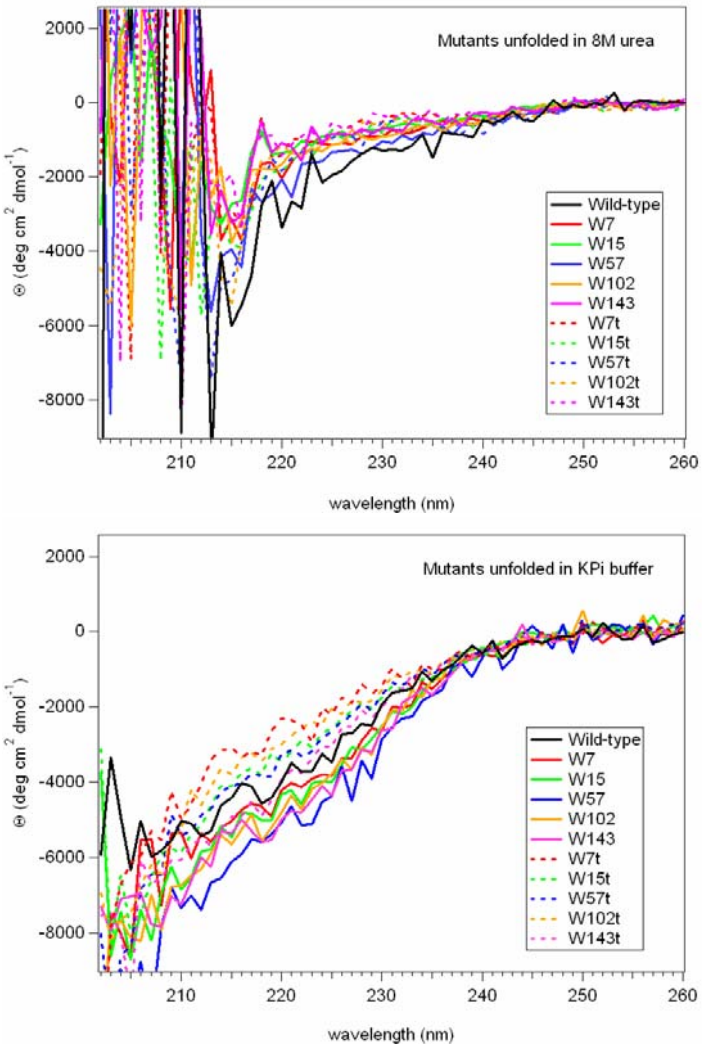

Figure 3.3. CD spectra of wild-type, full-length, and truncated Trp mutants unfolded in urea (top) and buffer (bottom).

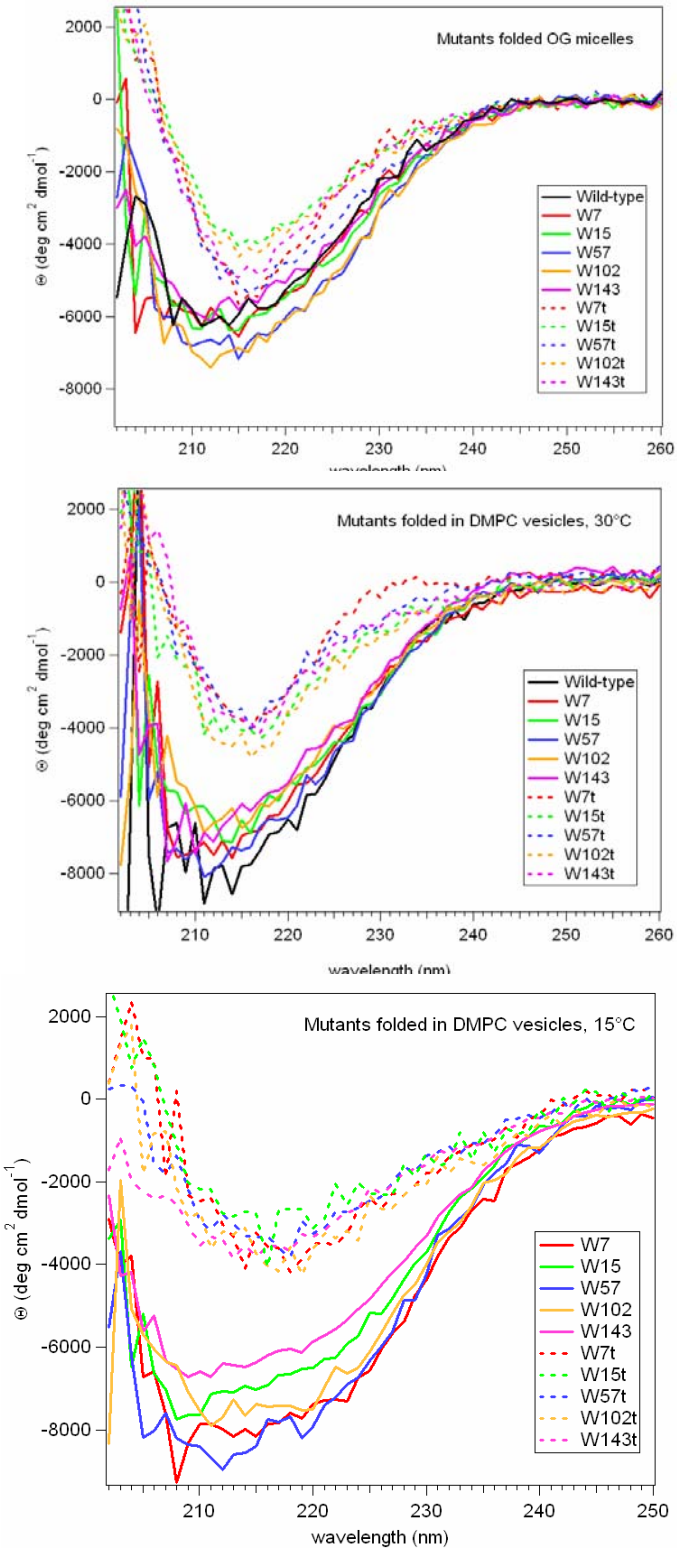

Figure 3.4. CD spectra of wild-type, full-length, and truncated Trp mutants folded in OG micelles (top), DMPC vesicles at 30 ^{o}C (middle), and DMPC vesicles at 15 ^{o}C (bottom).

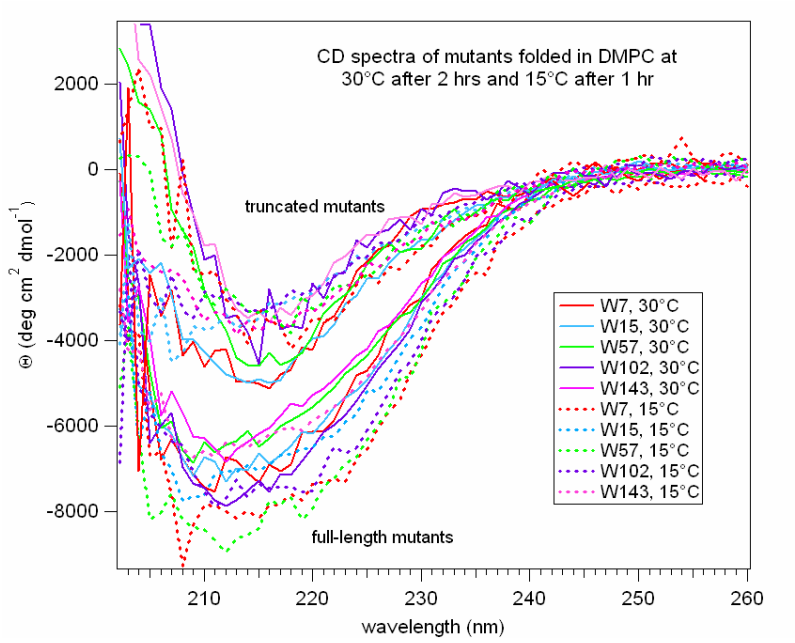

Figure 3.5. Overlay of CD spectra for Trp mutants at 30 ^{o}C (solid) and 15^{o}C (dotted). Truncated mutants display lower β-sheet signal than full-length. 15 ^{o}C data were averaged over the last 30-60 min of refolding. 30 ^{o}C data were averaged over 130-150 min into folding.

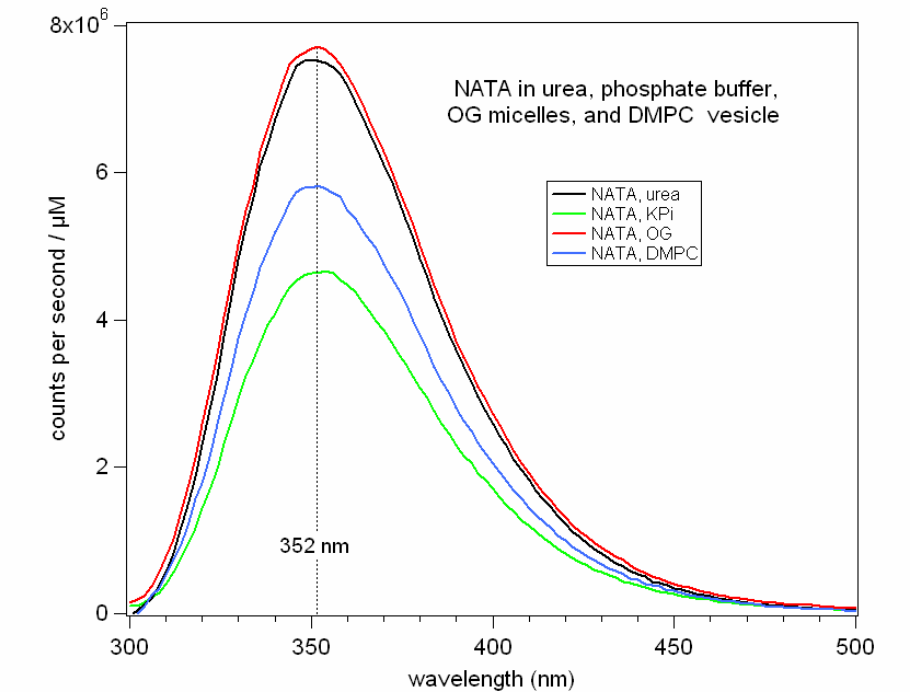

Figure 3.6. Steady-state fluorescence of NATA in urea, phosphate buffer, OG micelles, and DMPC vesicles at 30 ^{o}C. Spectra at 15 ^{o}C have the same emission maxima at 352 nm as the 30 ^{o}C spectra.

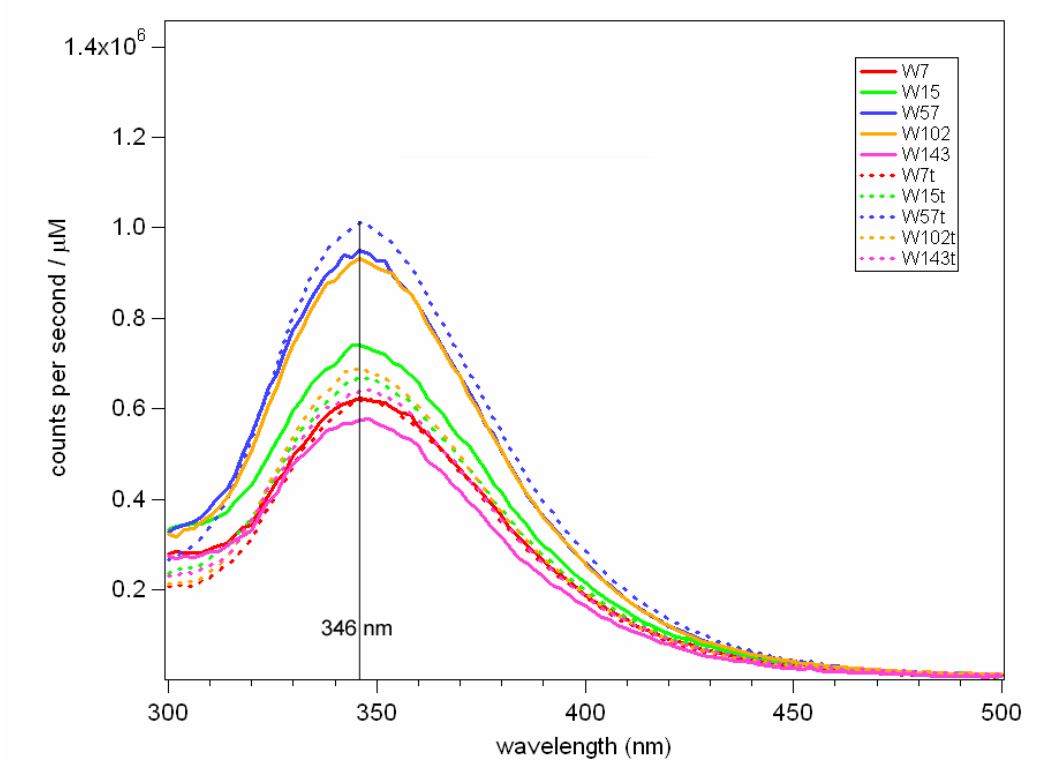

Figure 3.7. Steady-state fluorescence spectra of full-length (solid lines) and truncated (dotted lines) OmpA mutants unfolded in urea at 30 ^{o}C. Spectra were corrected for vesicle-only background and normalized to protein concentration.

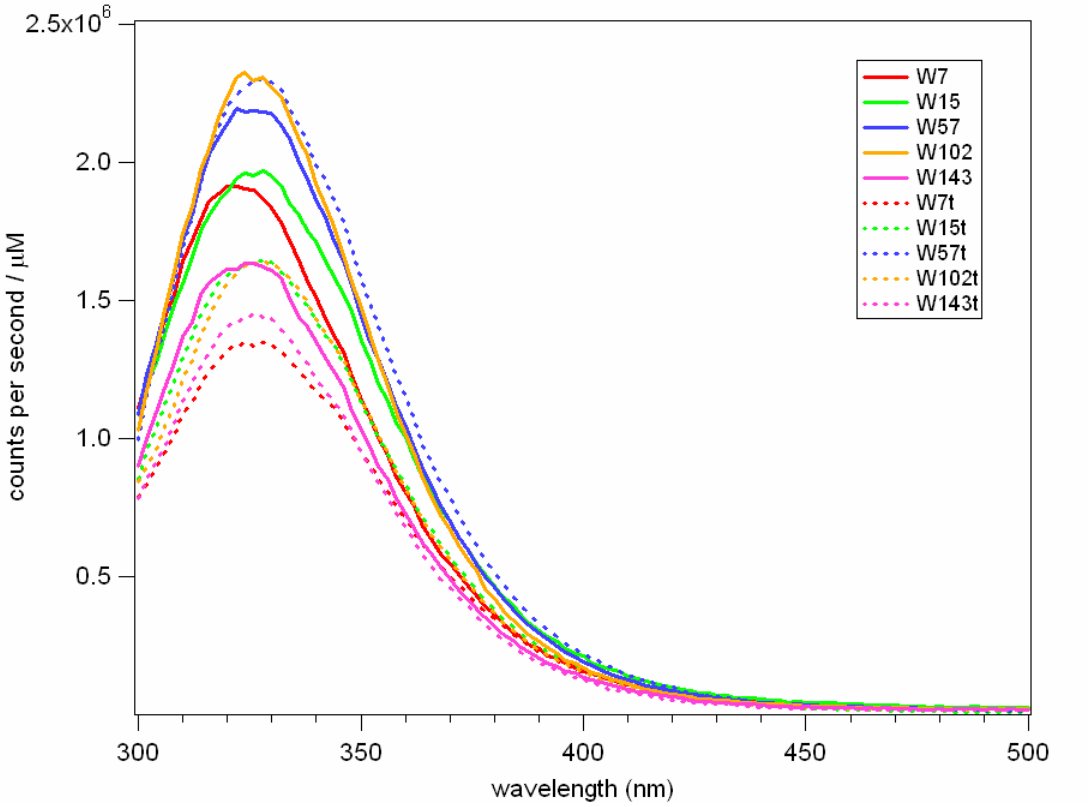

Figure 3.8. Steady-state fluorescence spectra of full-length (solid lines) and truncated (dotted lines) OmpA mutants folded in OG micelles at 30 ^{o}C. Spectra were corrected for vesicle-only background and normalized to protein concentration.

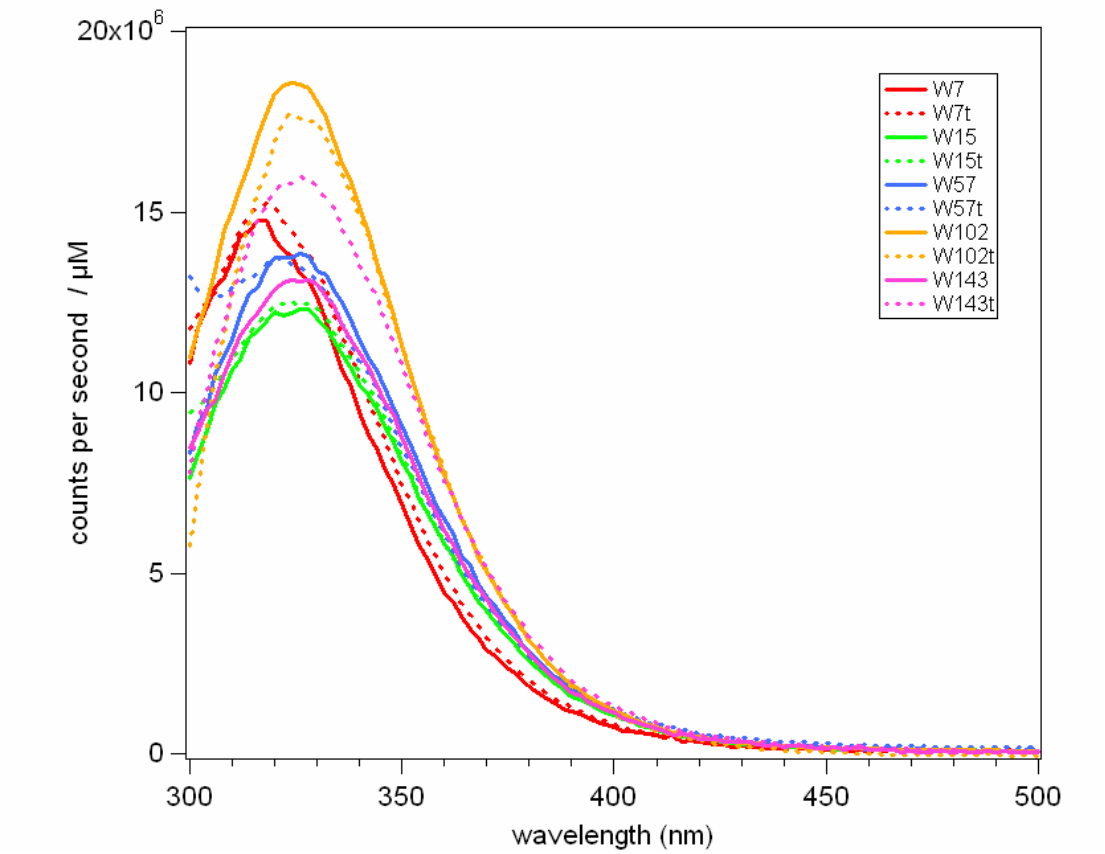

Figure 3.9. Steady-state fluorescence spectra of full-length (solid lines) and truncated OmpA mutants folded in DMPC vesicles at 30 ^{o}C. Spectra were corrected for vesicle-only background and normalized to protein concentration.

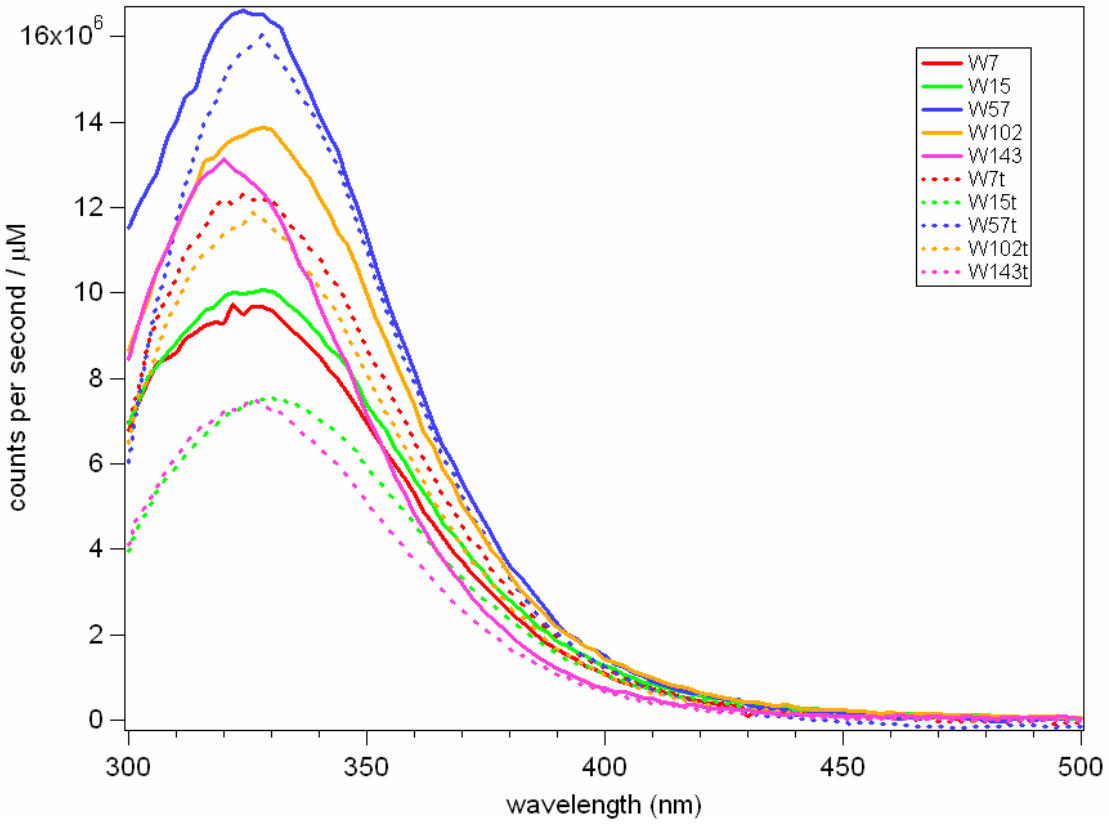

Figure 3.10. Steady-state fluorescence spectra of full-length (solid lines) and truncated (dotted lines) OmpA mutants folded in DMPC vesicles at 15 ^{o}C. Spectra were corrected for vesicle-only background and normalized to protein concentration.

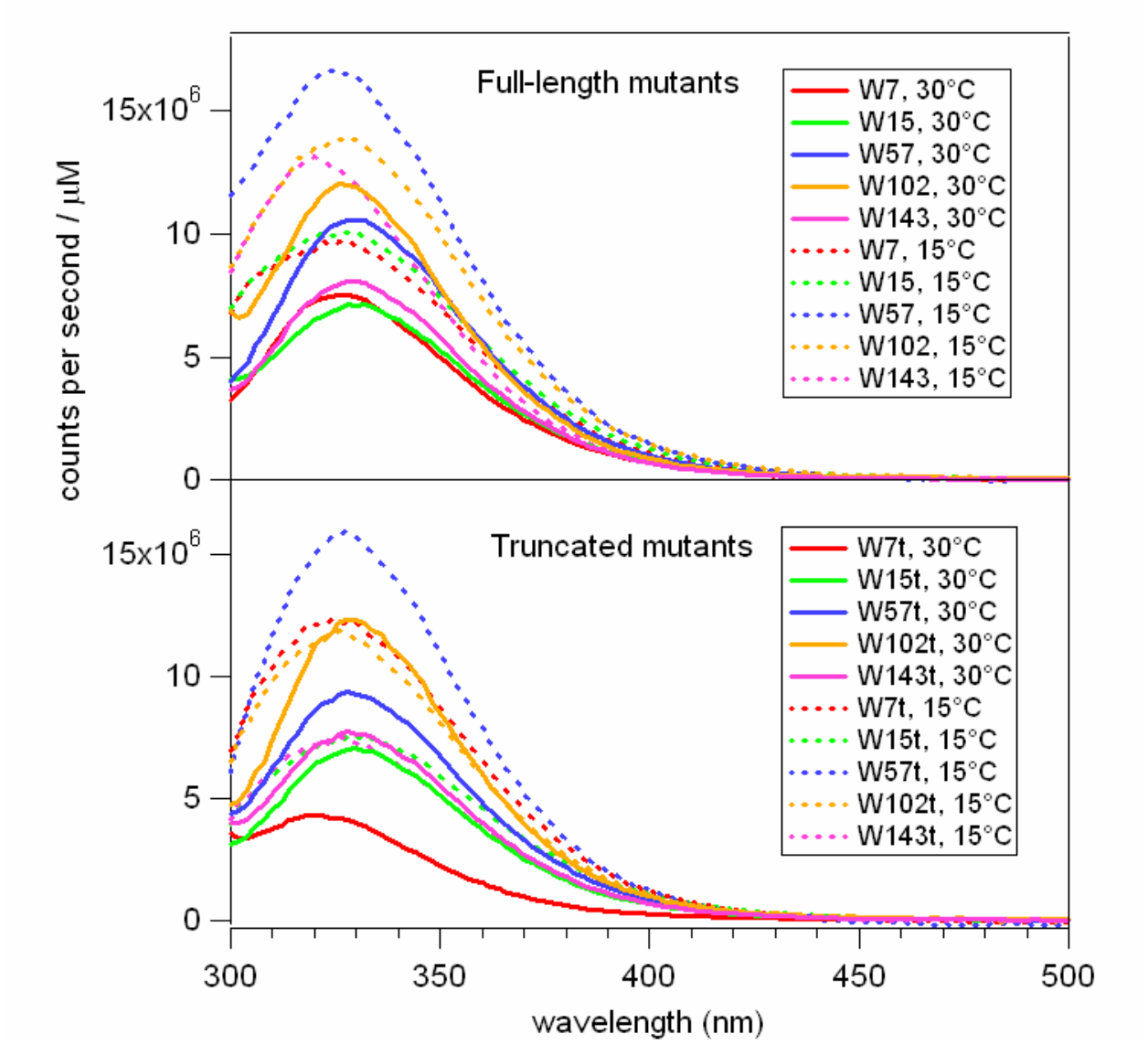

Figure 3.11. Comparison of steady-state fluorescence spectra of full-length and truncated OmpA mutants folded in DMPC vesicles at 30 °C (solid lines) and 15 °C (dotted lines). Top panel shows full-length mutants at both temperatures. Bottom panel shows truncated mutants at both temperatures. Spectra were corrected for vesicle-only background and normalized to protein concentration.

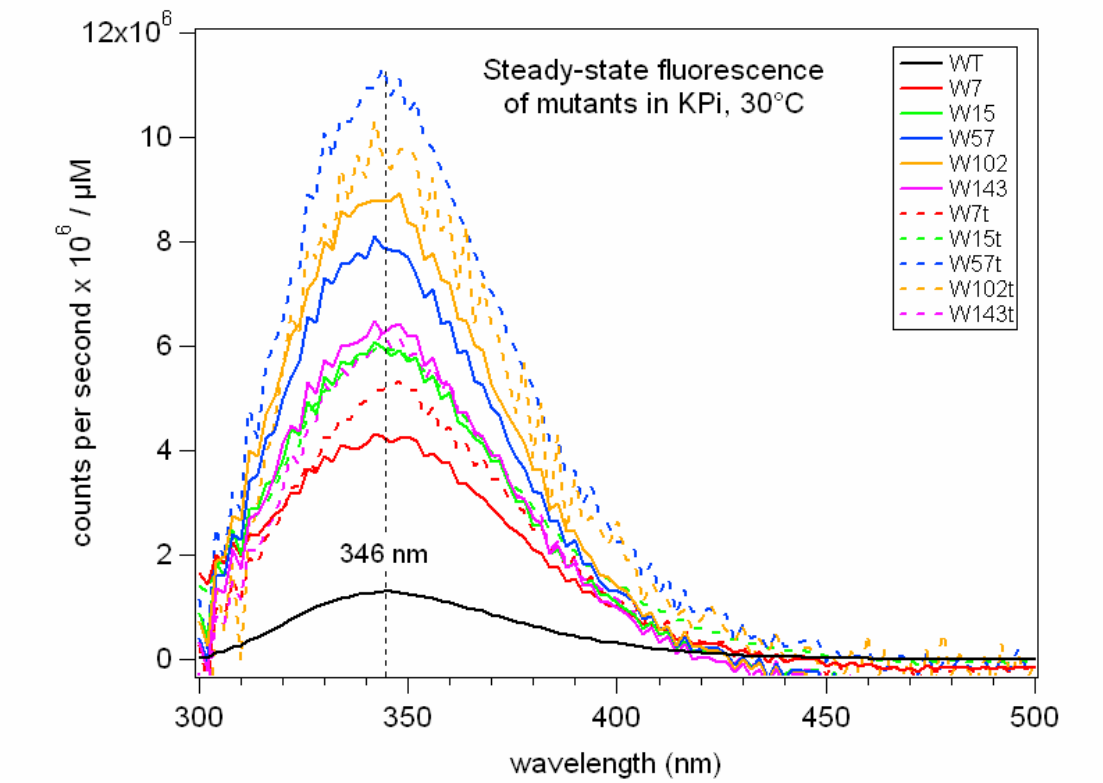

Figure 3.12. Steady-state fluorescence spectra of full-length (solid lines) and truncated (dotted lines) OmpA mutants unfolded in phosphate buffer at 30 ^{o}C. Spectra were corrected for vesicle-only background and normalized to protein concentration.

Mutant	Urea and KPi	OG micelles	DMPC vesicles
NATA	352	352	352
W7	346	322	318
W7t	346	324	318
W15	346	328	326
W15t	346	328	326
W57	346	324	325
W57t	346	326	325
W102	346	326	324
W102t	346	326	324
W143	346	326	326
W143t	346	326	327

Table 3.1 List of emission maxima for the different Trp mutants in urea, OG micelles, and DMPC vesicles in nm.

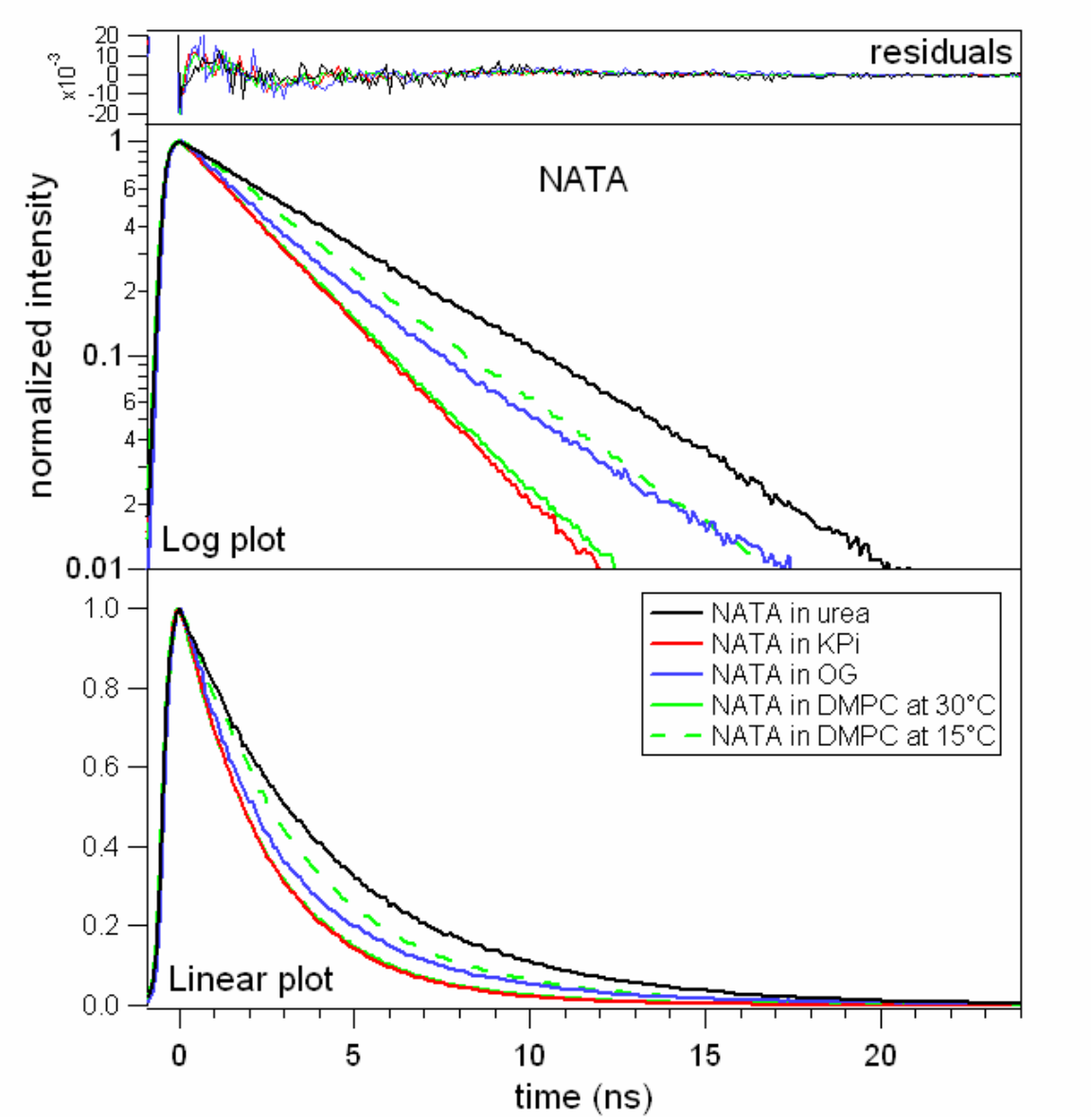

Figure 3.13 Time-resolved fluorescence of NATA in urea, phosphate buffer, micelles, and vesicles (30 ^{o}C and 15 ^{o}C).

NATA	amp1 (%)	τ_1 (ns)	amp2 (%)	τ_2 (ns)	amp3 (%)	τ_3 (ns)	weighted lifetimes (ns)
urea	61.9	4.7	32.0	3.5	6.1	6.6	4.4
KPi	100	2.5	---	---	---	---	2.5
OG	55.8	3.9	44	2.1	---	---	3.0
DMPC 30°C	54.4	2.8	45.6	2.4	---	---	2.6
DMPC 15°C	100	3.5	---	---	---	---	3.5

Table 3.2. Exponential (mono-, bi-, tri-) fits of lifetimes of NATA in urea, phosphate buffer, micelles, and vesicles (30 °C and 15 °C). Tryptophan decays were fit with triple exponentials. Amplitudes (amp) and their corresponding lifetimes (τ) are shown as well as the amplitude weighted lifetimes.

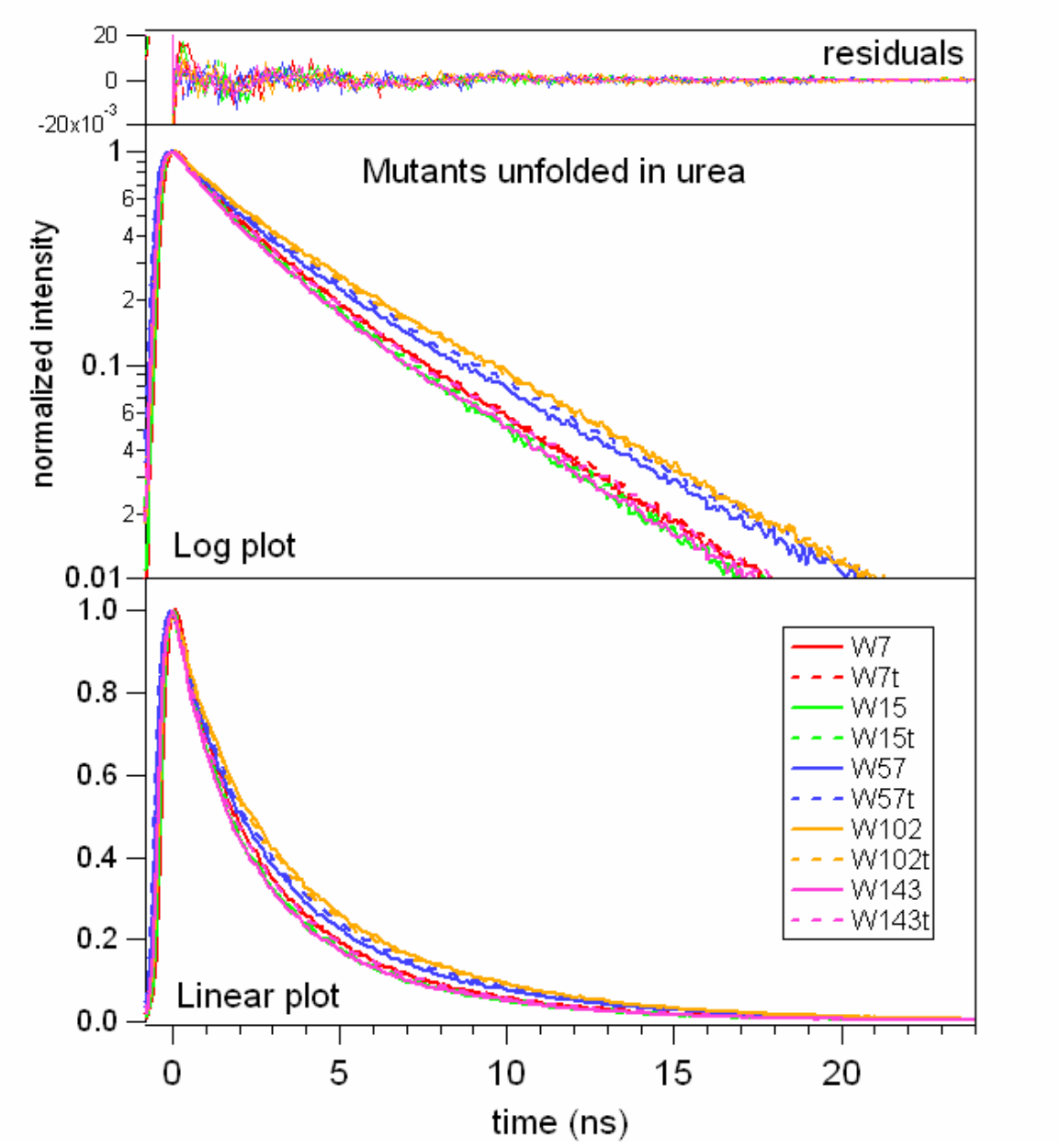

Figure 3.14. Time-resolved fluorescence of Trp mutants in urea.

Mutant	amp1 (%)	τ_1 (ns)	amp2 (%)	τ_2 (ns)	amp3 (%)	τ_3 (ns)	weighted lifetimes (ns)
W7	47	4.5	35	1.7	---	---	3.0
W7t	46	4.6	32	1.4	22	2.5	3.1
W15	45	4.4	54	1.7	---	---	2.9
W15t	47	4.4	40	1.5	13	2.1	3.0
W57	49	5.2	35	1.7	16	2.3	3.5
W57t	52	5.3	48	2.0	---	---	3.7
W102	59	5.2	41	1.9	---	---	3.9
W102t	57	5.3	44	1.9	---	---	3.8
W143	45	4.5	41	1.5	14	2.0	2.9
W143t	45	4.7	47	1.8	---	---	3.1

Table 3.3. Lifetimes of full-length and truncated mutants unfolded in urea. Tryptophan decays were fit to biexponentials or triple exponentials. Amplitudes (amp) and their corresponding lifetimes (τ) are shown as well as the amplitude weighted lifetimes.

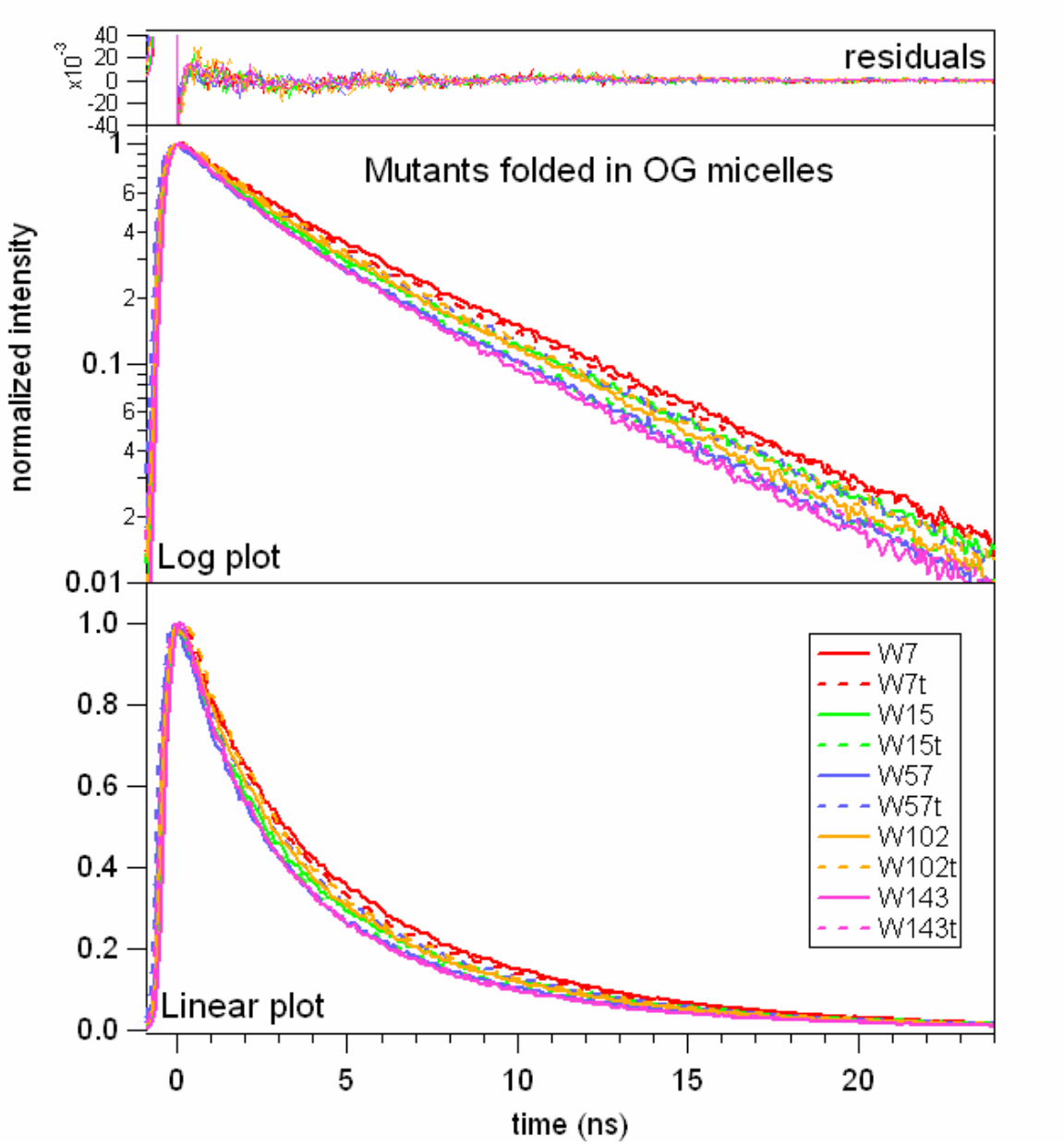

Figure 3.15. Time-resolved fluorescence of Trp mutants in OG micelles.

Mutant	amp1 (%)	τ_1 (ns)	amp2 (%)	τ_2 (ns)	amp3 (%)	τ_3 (ns)	weighted lifetimes (ns)
W7	63.4	6.6	36.6	2.5	---	---	5.1
W7t	56.6	6.5	33.2	2.3	10.2	2.7	4.7
W15	52.7	6.5	35.3	2.1	12.0	2.4	4.4
W15t	49.5	6.1	48	2.2	---	---	4.1
W57	52.0	5.9	48	2.0	---	---	4.0
W57t	62.0	6.0	30.6	2.0	7.4	2.4	4.5
W102	58.7	5.8	32.3	2.4	9.0	2.1	4.4
W102t	54.6	6.0	45.5	2.6	---	---	4.5
W143	51.9	5.5	35.3	1.9	12.8	2.1	3.8
W143t	51.2	5.8	48.9	2.0	---	---	3.9

Table 3.4. Lifetimes of full-length and truncated mutants folded in OG micelles. Tryptophan decays were fit to triple exponentials. Amplitudes (amp) and their corresponding lifetimes (τ) are shown as well as the weighted lifetimes.

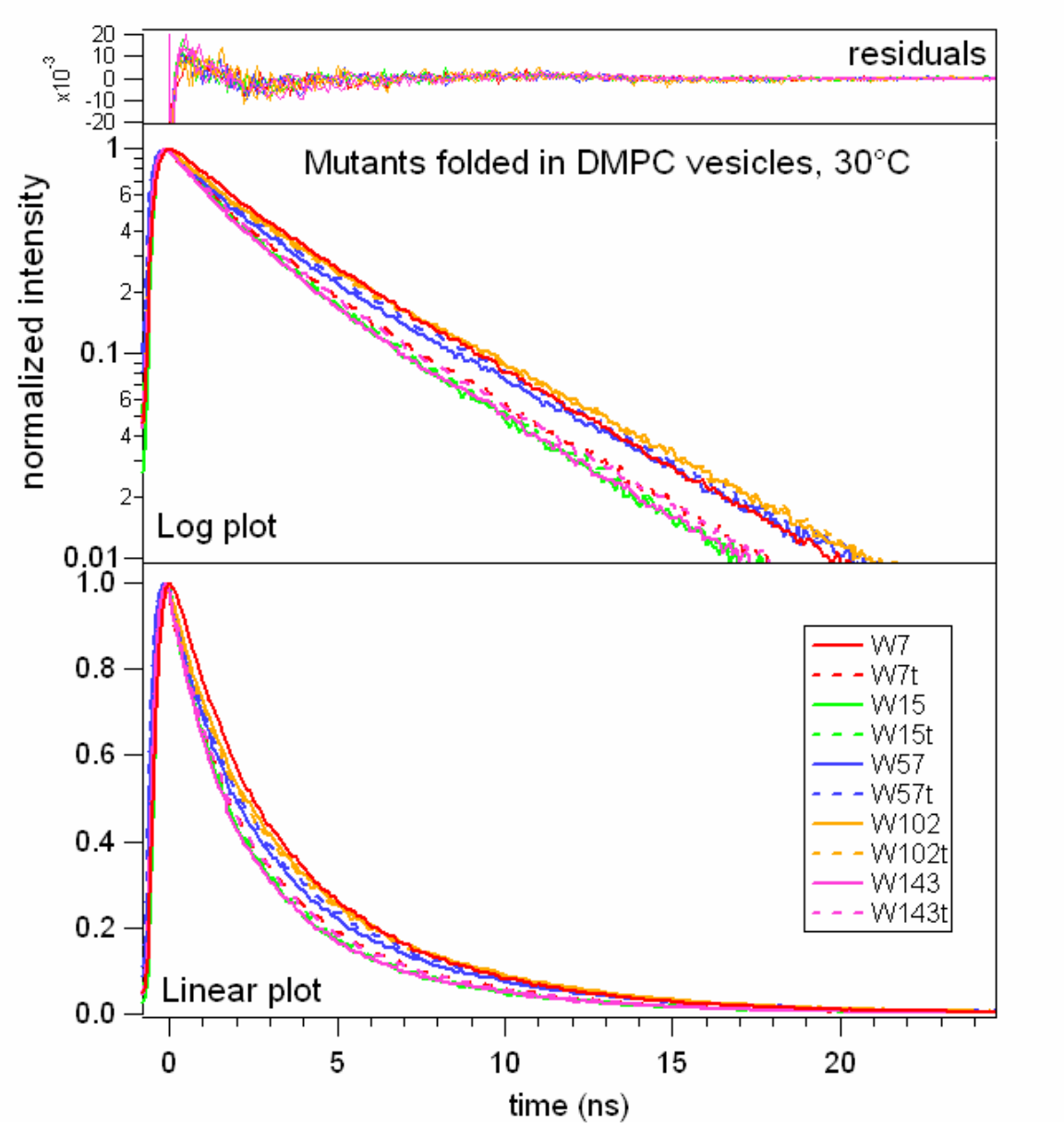

Figure 3.16. Time-resolved fluorescence of Trp mutants in DMPC vesicles, 30 ^{o}C.

Mutant	amp1 (%)	τ_1 (ns)	amp2 (%)	τ_2 (ns)	amp3 (%)	τ_3 (ns)	weighted lifetimes (ns)
W7	64.9	4.7	35.1	2.1	---	---	3.8
W7t	54.6	4.9	45.3	2.4	---	---	3.8
W15	46.4	5.7	53.6	2.2	---	---	3.9
W15t	44.7	5.4	55.3	2.1	---	---	3.6
W57	50.9	5.4	36.5	2.3	12.5	2.5	3.9
W57t	34.3	6.4	44.6	2.6	21.0	2.8	3.9
W102	55.4	5.5	34.2	2.5	10.3	2.1	4.1
W102t	55.8	5.8	44.2	2.7	---	---	4.4
W143	39.4	5.4	60.6	2.1	---	---	3.4
W143t	43.9	5.3	39.6	2.2	16.4	2.5	3.6

Table 3.5. Lifetimes of full-length and truncated mutants folded in DMPC vesicles at 30 ^{o}C. Tryptophan decays were fit to biexponentials or triple exponentials. Amplitudes (amp) and their corresponding lifetimes (τ) are shown as well as the weighted lifetimes.

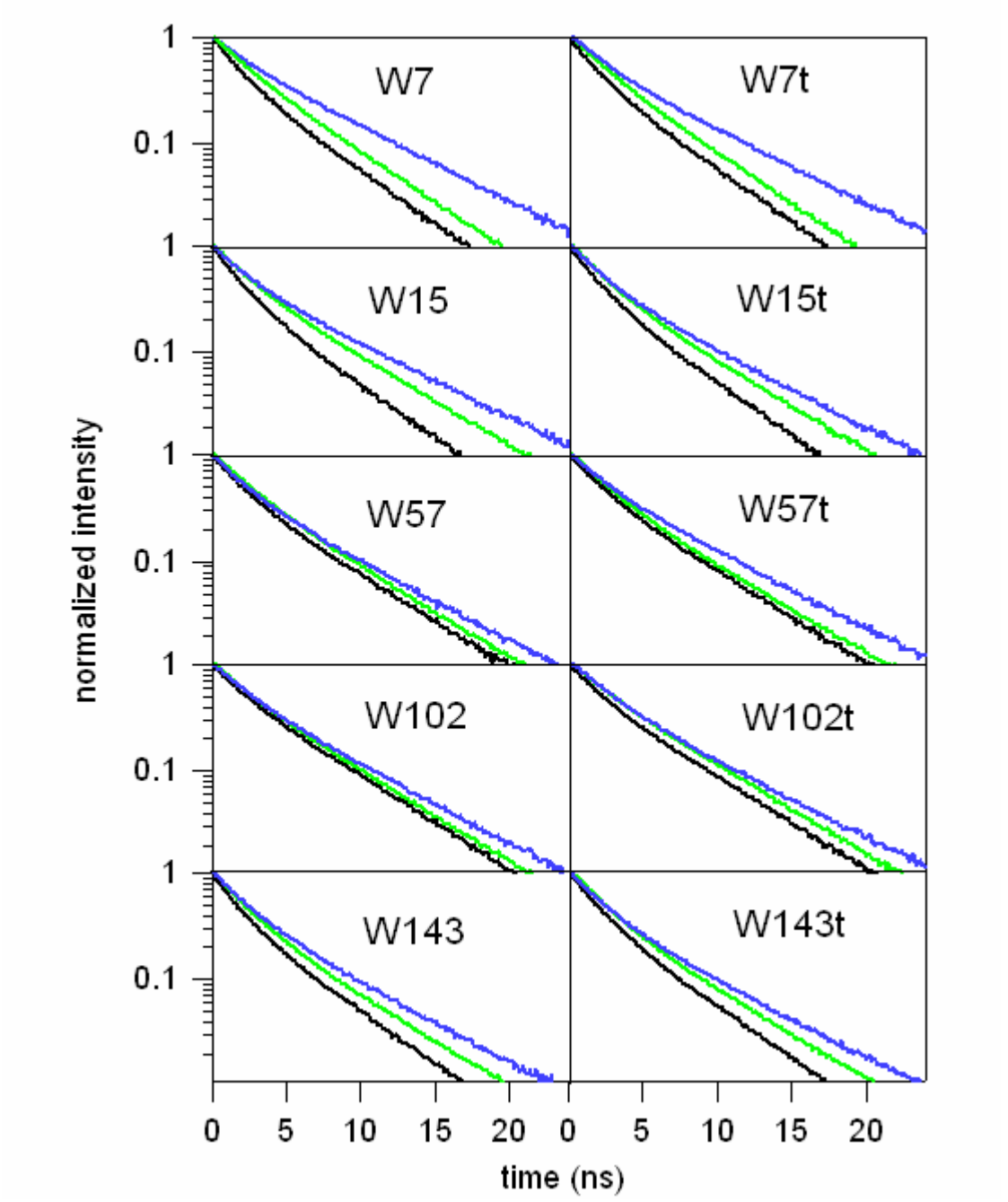

Figure 3.17. Fluorescence decays of full-length (left) and truncated mutants (right), mutants unfolded in urea (black), folded in OG micelles (blue), and folded in DMPC at 30 ^{o}C (green).

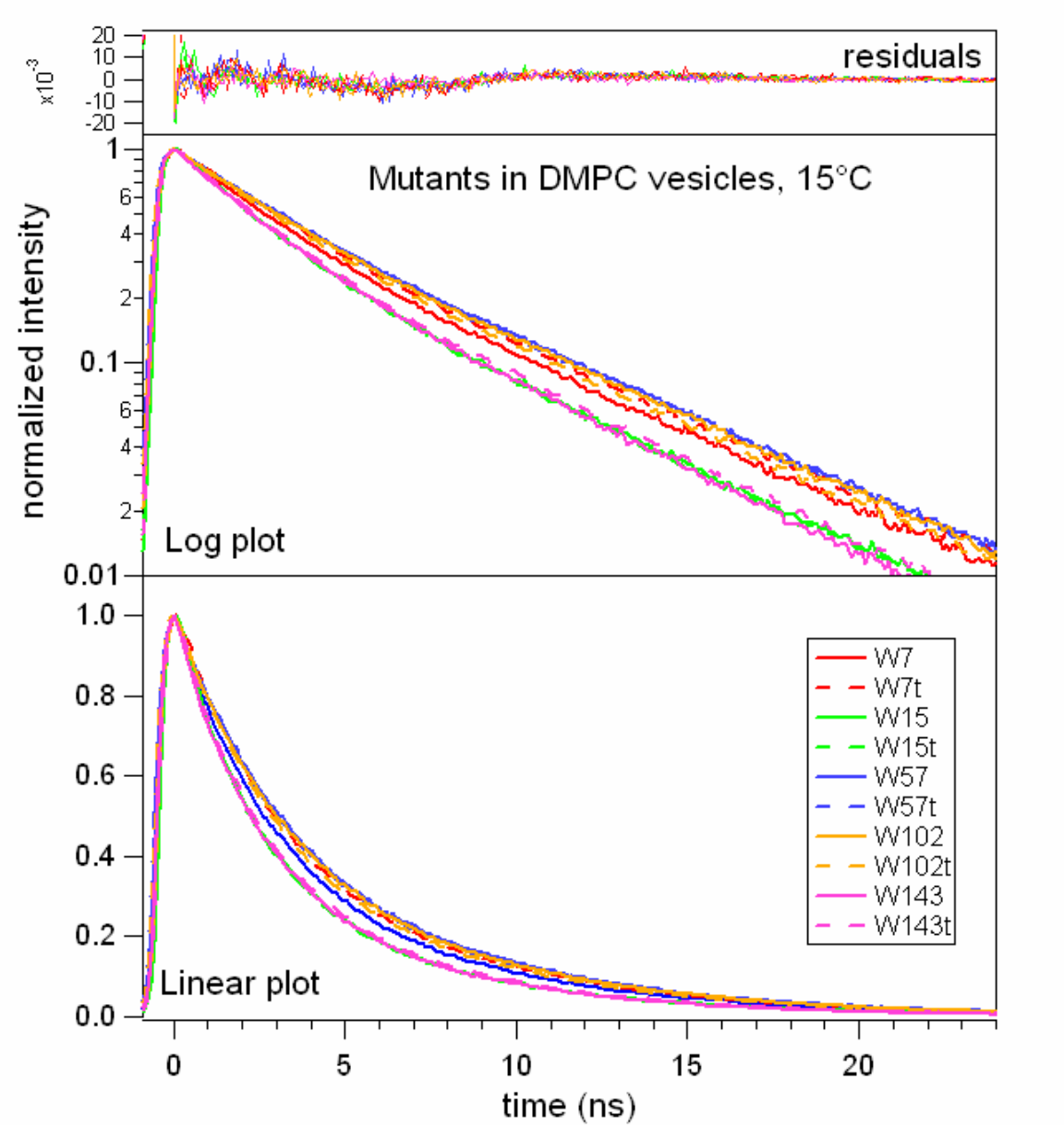

Figure 3.18. Time-resolved fluorescence of Trp mutants in DMPC vesicles, 15 ^{o}C

Mutant	amp1 (%)	τ_1 (ns)	amp2 (%)	τ_2 (ns)	weighted lifetimes (ns)
W7	43	5.6	57	2.6	3.9
W7t	40	7.2	60	3.0	4.7
W15	38	6.0	62	2.2	3.6
W15t	37	6.0	63	2.2	3.6
W57	46	7.0	54	3.1	4.9
W57t	42	7.1	58	3.1	4.8
W102	50	6.7	50	2.0	4.4
W102t	43	6.8	57	2.9	4.6
W143	43	5.7	57	2.2	3.7
W143t	40	6.2	60	2.3	3.9

Table 3.6. Lifetimes of full-length and truncated mutants folded in DMPC vesicles at 15 ^{o}C. Tryptophan decays were fitted to biexponentials. Amplitudes (amp) and their corresponding lifetimes (τ) are shown as well as the weighted lifetimes.

	average lifetimes (ns)		
sample	**urea**	**OG micelles**	**DMPC vesicles**
NATA	4.4	3.0	2.6
W7	3.3	5.1	3.8
W7t	3.1	4.7	3.8
W15	2.9	4.5	3.8
W15t	2.9	4.2	3.6
W57	3.5	4.0	3.9
W57t	3.7	4.5	3.9
W102	3.8	4.4	4.1
W102t	3.8	4.5	4.4
W143	2.9	3.8	3.4
W143t	3.2	3.9	3.6

Table 3.7. List summarizing the amplitude weighted lifetimes of NATA and Trp mutants in urea, micelles, and vesicles.

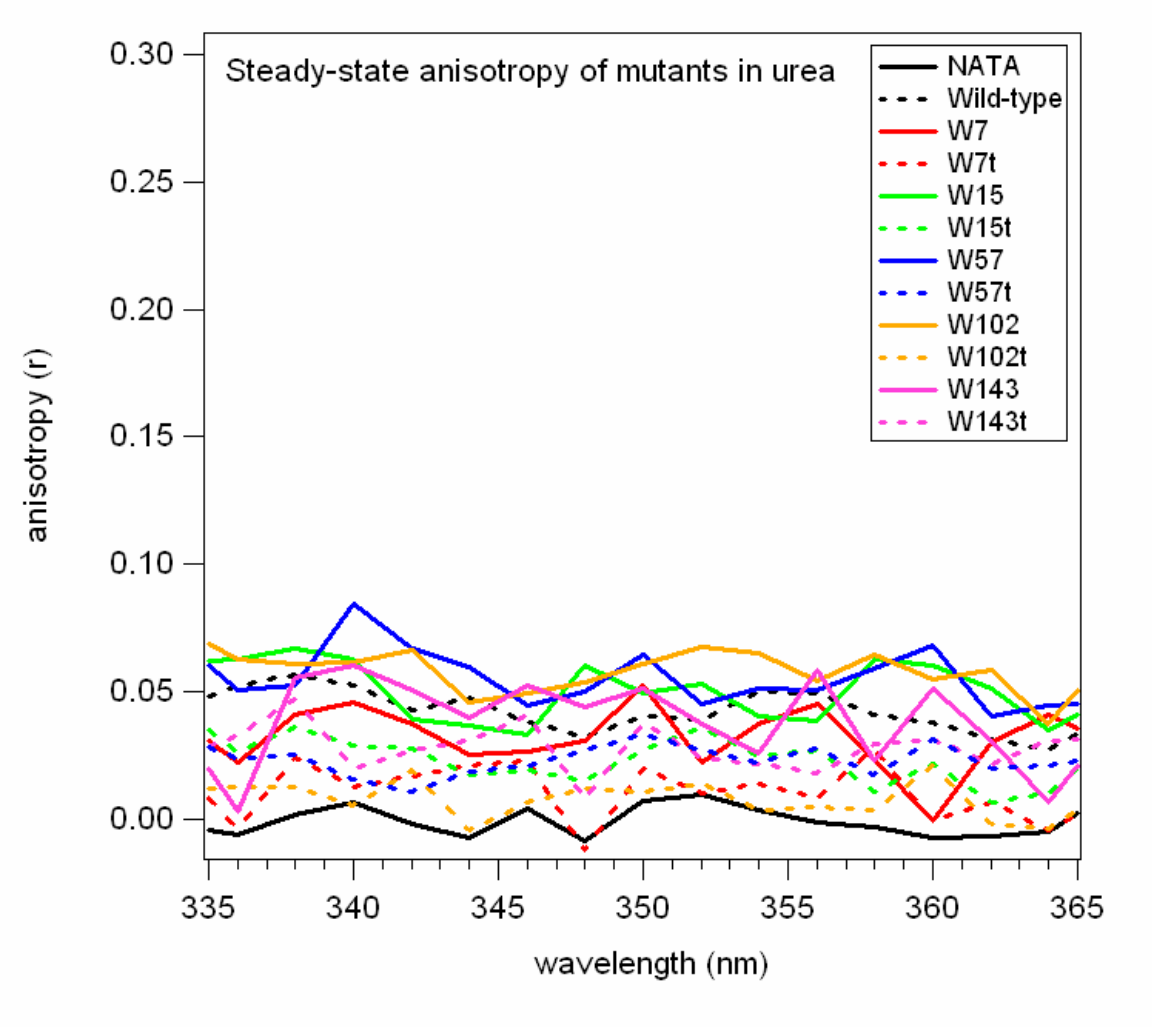

Figure 3.19. Steady-state anisotropy of mutants in urea.

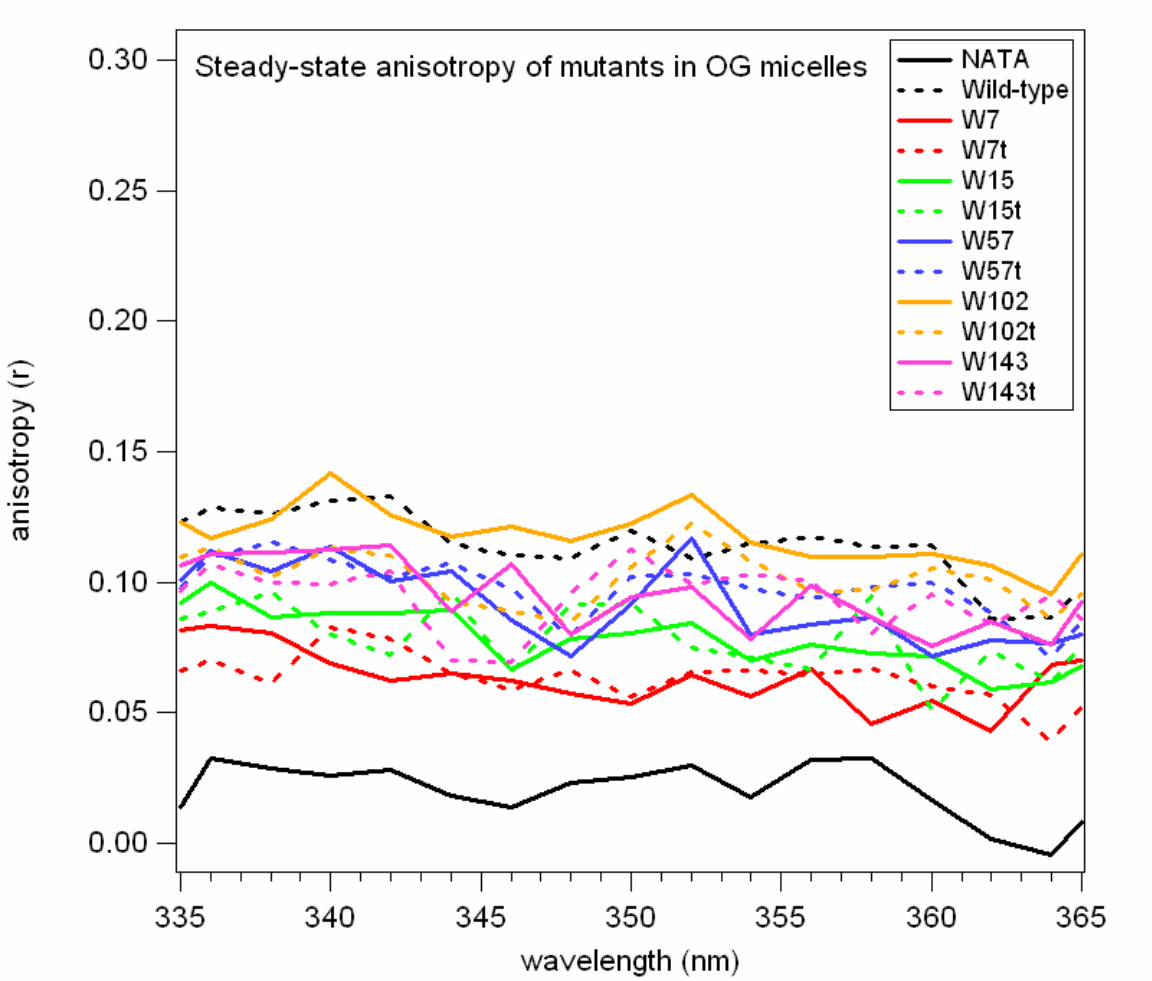

Figure 3.20. Steady-state anisotropy of mutants in micelles.

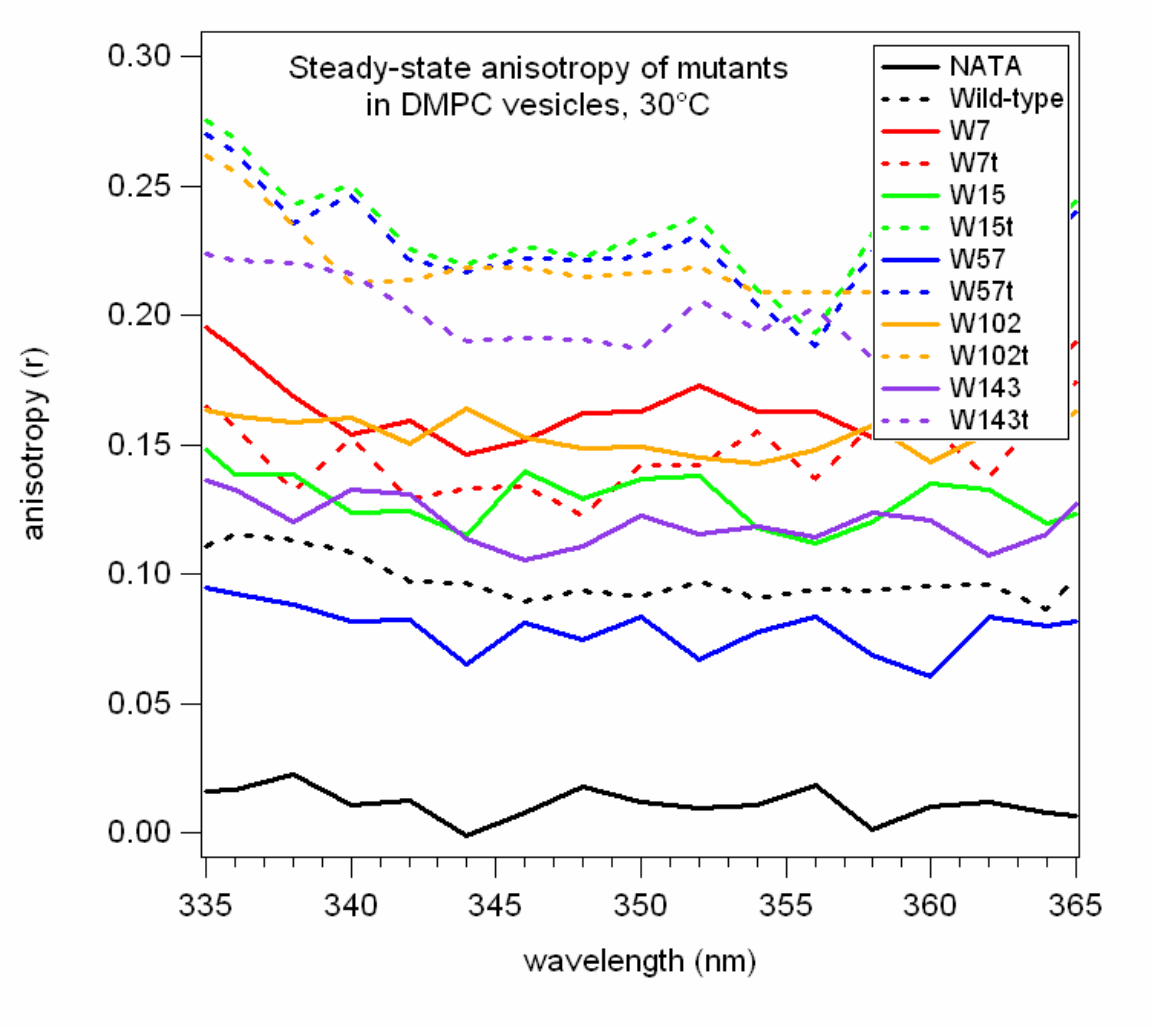

Figure 3.21. Steady-state anisotropy of mutants in DMPC.

	steady-state anisotropy (r)		
sample	**urea**	**OG micelles**	**DMPC vesicles**
NATA	0.00	.02	<0.01
WT	0.04	0.11	<0.10
W7	0.03	0.06	<0.17
W7t	0.03	0.06	<0.14
W15	0.05	0.08	<0.13
W15t	0.02	0.08	<0.23
W57	0.06	0.09	<0.08
W57t	0.02	0.10	<0.23
W102	0.06	0.12	<0.15
W102t	0.01	0.10	<0.22
W143	0.04	0.09	<0.12
W143t	0.03	0.09	<0.20

Table 3.8. Steady-state anisotropy of NATA and Trp mutants in urea, OG micelles, and DMPC vesicles (30^{o}C).

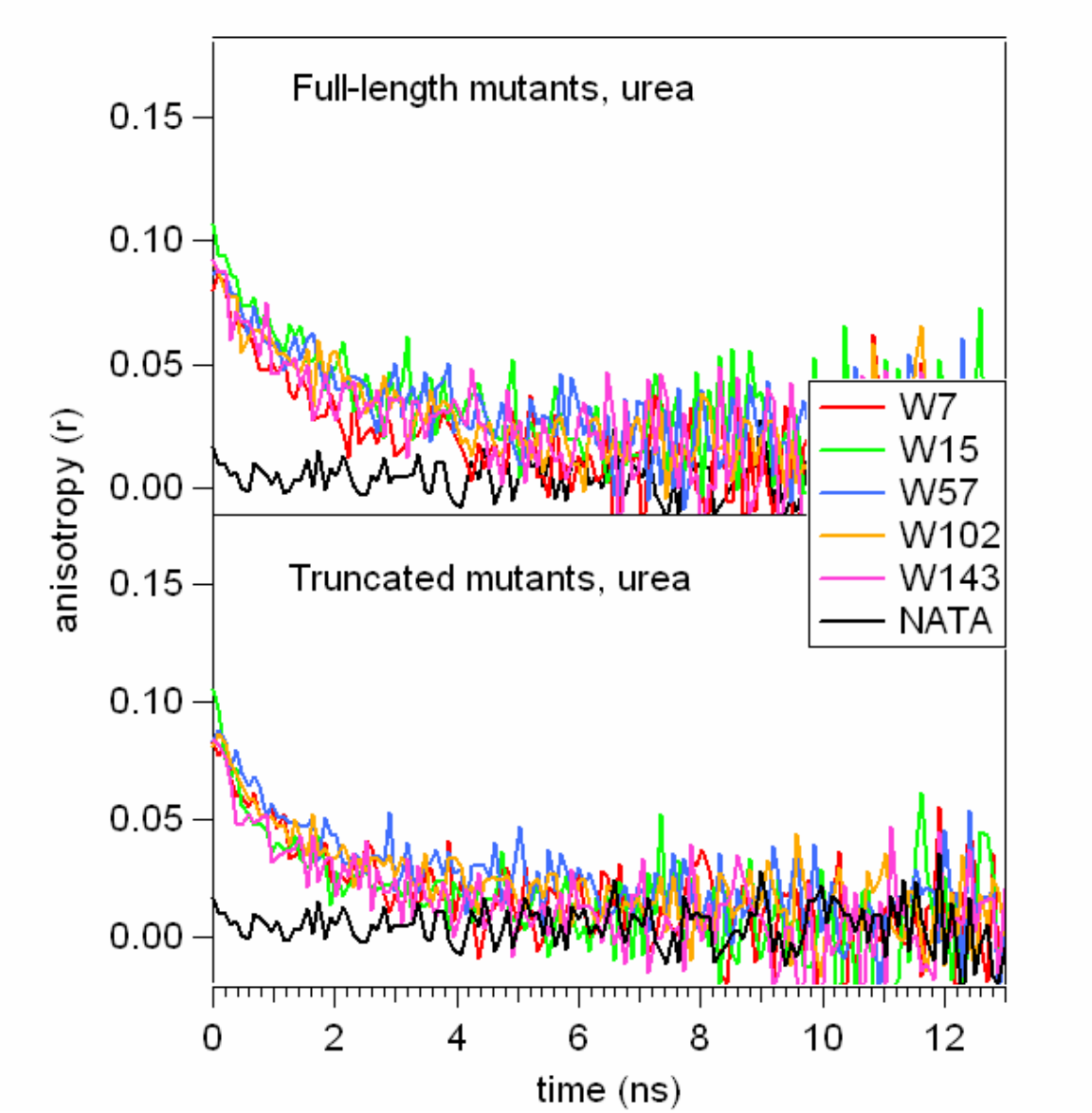

Figure 3.22. Time-resolved anisotropy of full-length (top) and truncated mutants (bottom) unfolded in urea. Measurements were taken in a 50 ns time window.

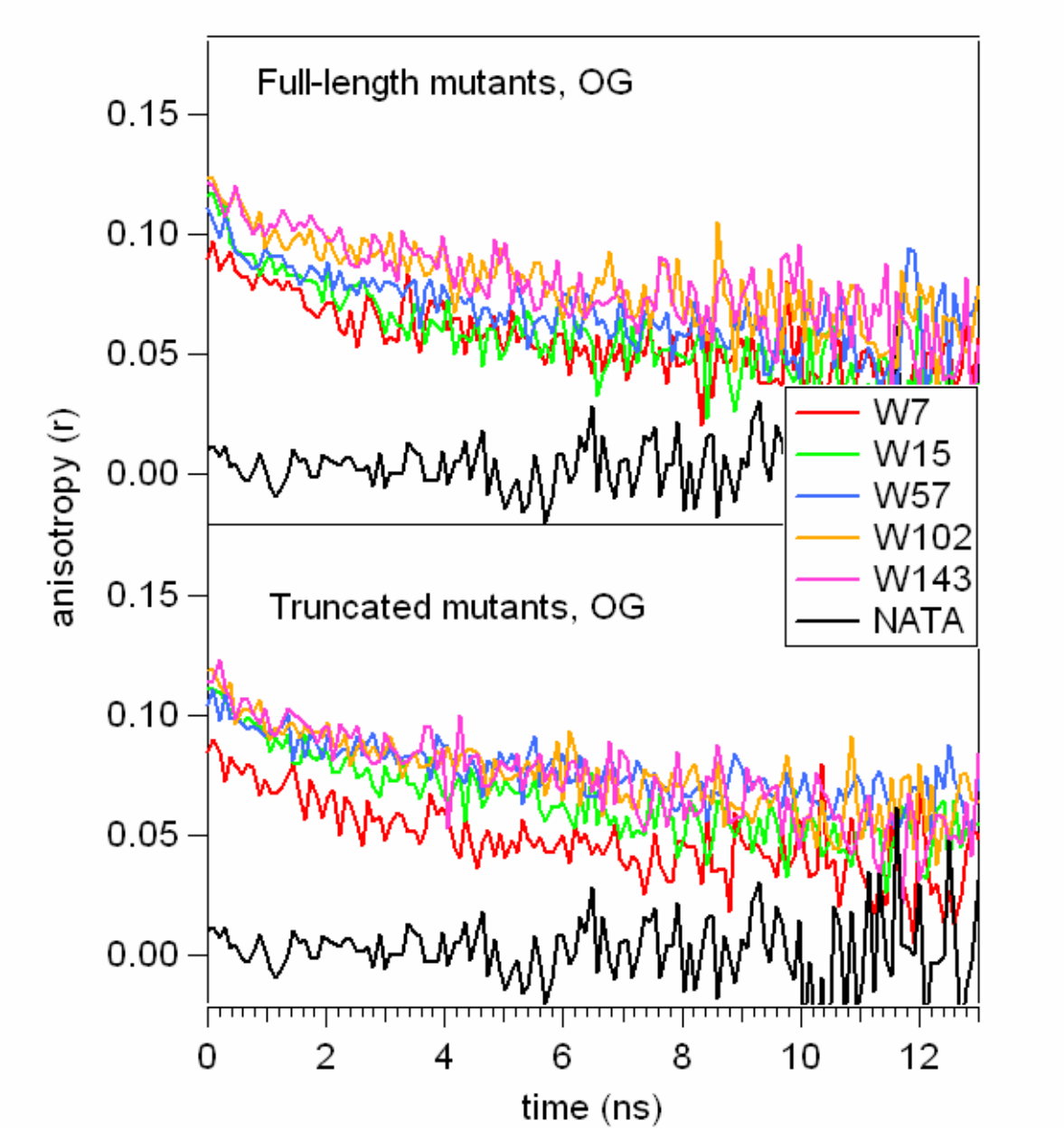

Figure 3.23. Time-resolved anisotropy of full-length (top) and truncated mutants (bottom) folded in OG micelles. Measurements were taken in a 50 ns time window.

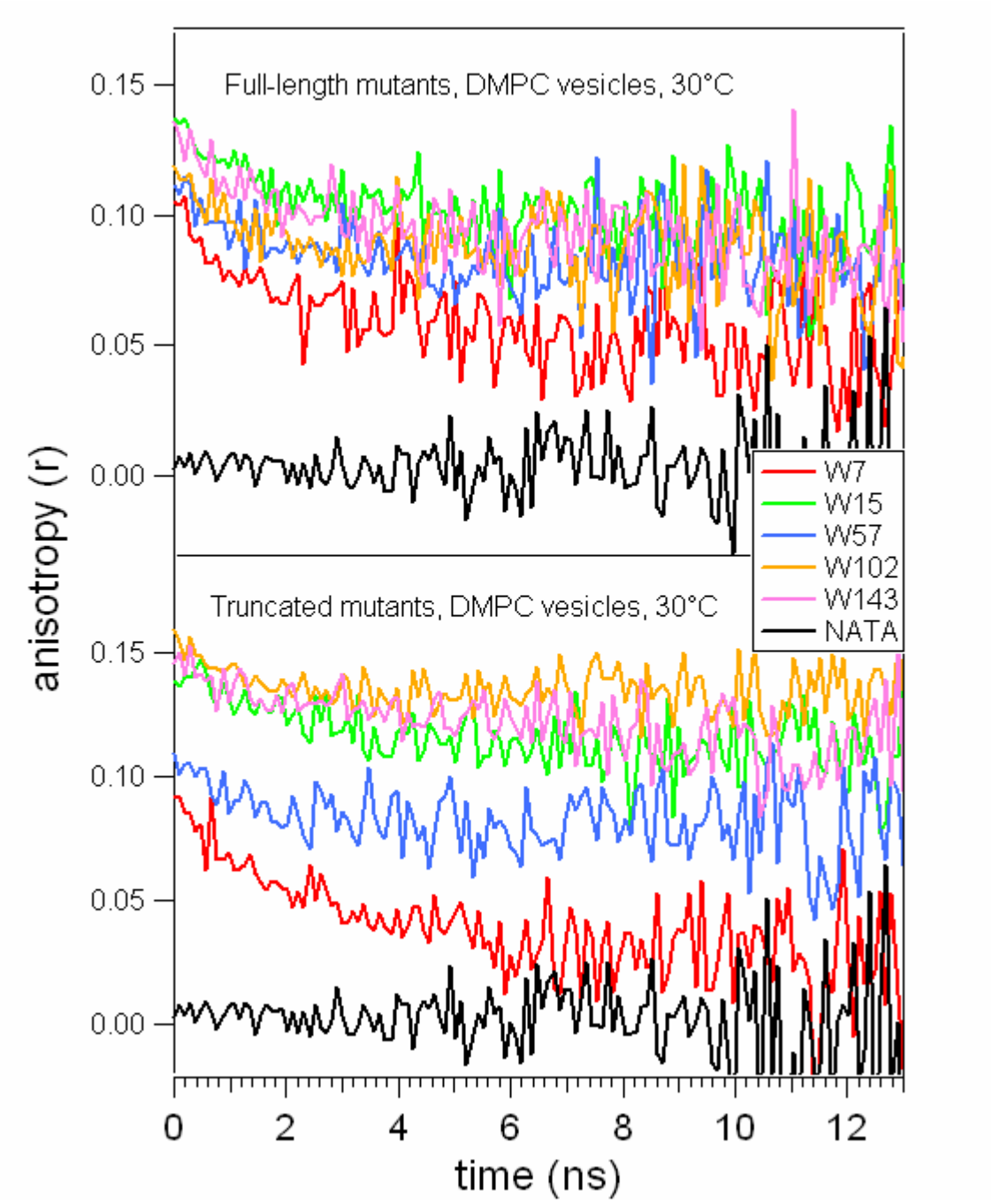

Figure 3.24. Time-resolved anisotropy of full-length (top) and truncated mutants (bottom) folded in DMPC vesicles at 30 ^{o}C. Measurements were taken in a 50 ns time window.

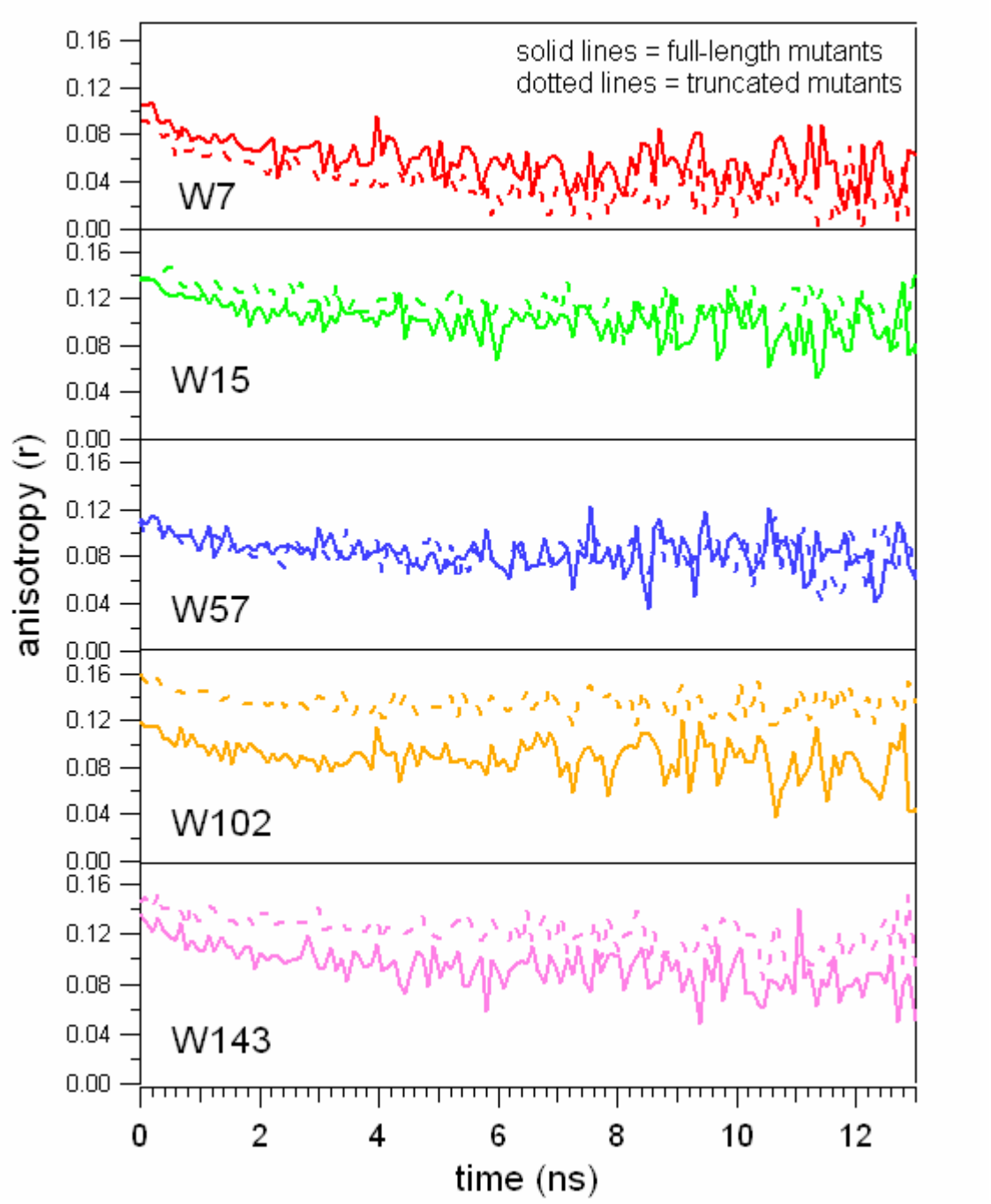

Figure 3.25 Overlay of anisotropy decays for full-length and truncated mutants for each Trp position.

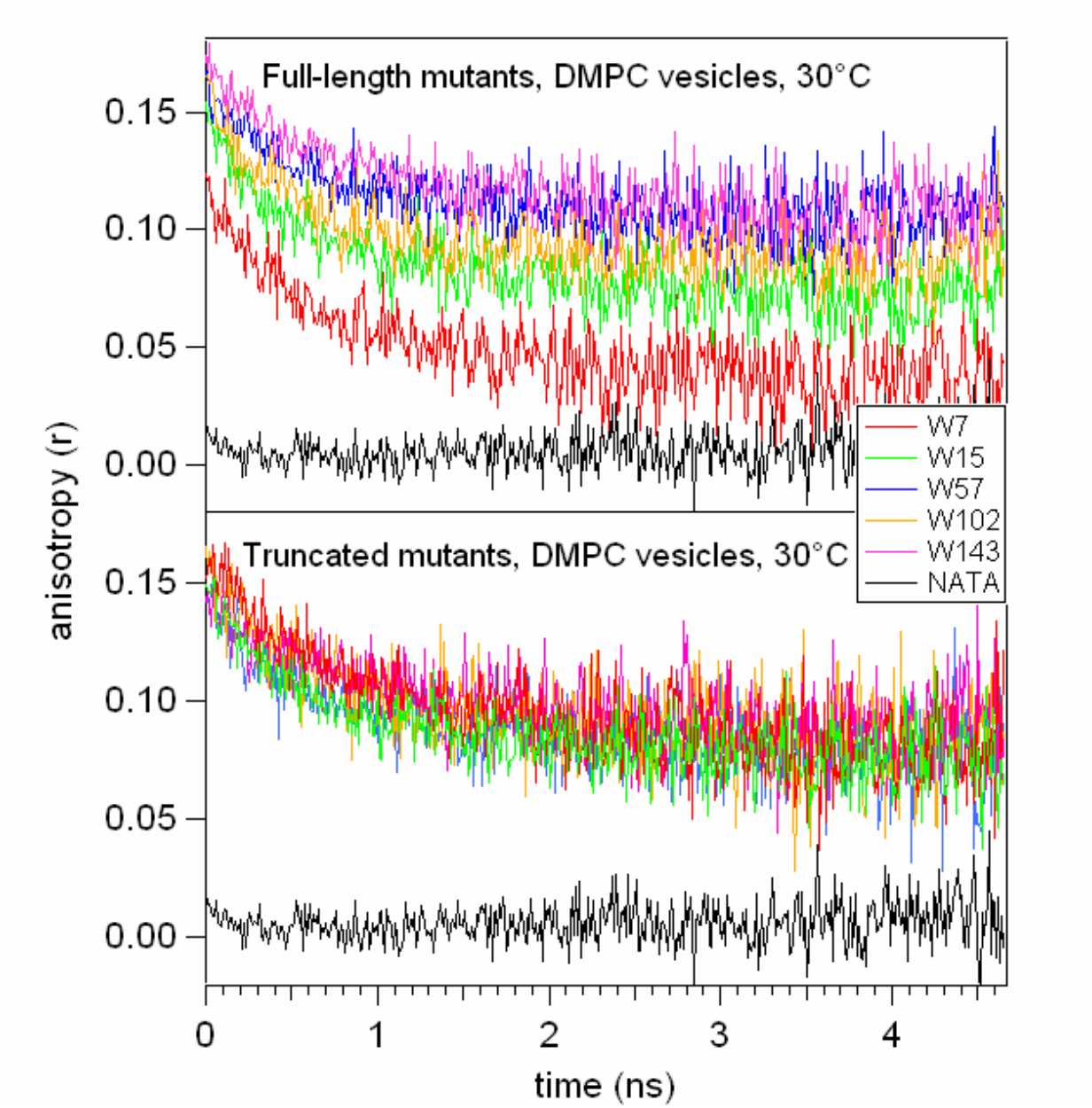

Figure 3.26. Time-resolved anisotropy of full-length (top) and truncated mutants (bottom) folded in DMPC vesicles at 30 °C. Measurements were taken in a 5 ns time window.

Protein environment	Average fast Θ_1	Average slow Θ_2
Urea	0.9 ns	6 ns
OG micelles	2 ns	11 ns
DMPC vesicles	2 ns	26 ns

Table 3.9. Average slow and fast correlation times (Θ) for both full-length and truncated mutants.

3.5 REFERENCES

Arora, A., Rinehart, D., Szabo, G., and Tamm, L. K. (2000) Refolded outer membrane protein A of Escherichia coli forms ion channels with two conductance states in planar lipid bilayers, *Journal of Biological Chemistry 275*, 1594-1600.

Arora, A., Abildgaard, F., Bushweller, J. H., and Tamm, L. K. (2001) Structure of outer membrane protein A transmembrane domain by NMR spectroscopy, *Nature Structural Biology 8*, 334-338.

Beechem, J. M., and Brand, L. (1985) Time-resolved fluorescence of proteins, *Annual Review of Biochemistry 54*, 43-71.

Beychok, S. (1966) Circular dichroism of biological macromolecules, *Science 154*, 1288-&.

Brown, M. F., Seelig, J., and Haberlen, U. (1979) Structural dynamics in phospholipid-bilayers from deuterium spin-lattice relaxation-time measurements, *Journal of Chemical Physics 70*, 5045-5053.

Chen, Y., and Barkley, M. D. (1998) Toward understanding tryptophan fluorescence in proteins, *Biochemistry 37*, 9976-9982.

Clayton, A. H. A., and Sawyer, W. H. (2000) Site-specific tryptophan dynamics in class A amphipathic helical peptides at a phospholipid bilayer interface, *Biophysical Journal 79*, 1066-1073.

Cowan, S. W., and Rosenbusch, J. P. (1994) Folding pattern diversity of integral membrane-proteins, *Science 264*, 914-916.

Doring, K., Konermann, L., Surrey, T., and Jahnig, F. (1995) A long lifetime component in the tryptophan fluorescence of some proteins, *European Biophysics Journal 23*, 423-432.

Dornmair, K., Kiefer, H., and Jahnig, F. (1990) Refolding of an integral membrane-protein - OmpA of *Escherichia-coli*, *Journal of Biological Chemistry 265*, 18907-18911.

Greenfield, N. J. (1996) Methods to estimate the conformation of proteins and polypeptides from circular dichroism data, *Analytical Biochemistry 235*, 1-10.

Kleinschmidt, J. H., den Blaauwen, T., Driessen, A. J. M., and Tamm, L. K. (1999) Outer membrane protein A of Escherichia coli inserts and folds into lipid bilayers by a concerted mechanism, *Biochemistry 38*, 5006-5016.

Kleinschmidt, J. H., and Tamm, L. K. (2002) Secondary and tertiary structure formation of the beta-barrel membrane protein OmpA is synchronized and depends on membrane thickness, *Journal of Molecular Biology 324*, 319-330.

Lakowicz, J. R. (1999) *Principles of fluorescence spectroscopy*, 2nd edition ed., Kluwer Academic/Plenum Publishers, New York, NY.

Lami, H., and Glasser, N. (1986) Indole solvatochromism revisited, *Journal of Chemical Physics 84*, 597-604.

Lovejoy, C., Holowka, D. A., and Cathou, R. E. (1977) Nanosecond fluorescence spectroscopy of pyrenebutyrate anti-pyrene antibody complexes, *Biochemistry 16*, 3668-3672.

Mendelso.Ra, Morales, M. F., and Botts, J. (1973) Segmental flexibility of S-1 moiety of myosin, *Biochemistry 12*, 2250-2255.

Munro, I., Pecht, I., and Stryer, L. (1979) Sub-nanosecond motions of tryptophan residues in proteins, *Proceedings of the National Academy of Sciences of the United States of America 76*, 56-60.

O'Connor, D. V., and Phillips, D. (1984) *Time-Correlated Single Photon Counting*, Academic Press.

Pautsch, A., and Schulz, G. E. (1998) Structure of the outer membrane protein A transmembrane domain, *Nature Structural Biology 5*, 1013-1017.

Pautsch, A., and Schulz, G. E. (2000) High-resolution structure of the OmpA membrane domain, *Journal of Molecular Biology 298*, 273-282.

Pletneva, E. V., Gray, H. B., and Winkler, J. R. (2005) Many faces of the unfolded state: Conformational heterogeneity in denatured yeast cytochrome *c*, *Journal of Molecular Biology 345*, 855-867.

Rodionova, N. A., Tatulian, S. A., Surrey, T., Jahnig, F., and Tamm, L. K. (1995) Characterization of 2 membrane-bound forms of OmpA, *Biochemistry 34*, 1921-1929.

Ruggiero, A. J., Todd, D. C., and Fleming, G. R. (1990) Subpicosecond fluorescence anisotropy studies of tryptophan in water, *Journal of the American Chemical Society 112*, 1003-1014.

Schiffer, M., Chang, C. H., and Stevens, F. J. (1992) The functions of tryptophan residues in membrane-proteins, *Protein Engineering 5*, 213-214.

Sugawara, E., and Nikaido, H. (1994) OmpA protein of *Escherichia-coli* outer-membrane occurs in open and closed channel forms, *Journal of Biological Chemistry 269*, 17981-17987.

Surrey, T., and Jahnig, F. (1992) Refolding and oriented insertion of a membrane-protein into a lipid bilayer, *Proceedings of the National Academy of Sciences of the United States of America 89*, 7457-7461.

Surrey, T., and Jahnig, F. (1995) Kinetics of folding and membrane insertion of a beta-barrel membrane protein, *Journal of Biological Chemistry 270*, 28199-28203.

Surrey, T., Schmid, A., and Jahnig, F. (1996) Folding and membrane insertion of the trimeric beta-barrel protein OmpF, *Biochemistry 35*, 2283-2288.

Szabo, A. G., and Rayner, D. M. (1980) The time-resolved emission-spectra of peptide conformers measured by pulsed laser excitation, *Biochemical and Biophysical Research Communications 94*, 909-915.

Toptygin, D., Savtchenko, R. S., Meadow, N. D., Roseman, S., and Brand, L. (2002) Effect of the solvent refractive index on the excited-state lifetime of a single tryptophan residue in a protein, *Journal of Physical Chemistry B 106*, 3724-3734.

Valeur, B., and Weber, G. (1977) Resolution of fluorescence excitation spectrum of indole into 1LA and 1LH excitation bands, *Photochemistry and Photobiology 25*, 441-444.

Vogel, H., and Jahnig, F. (1986) Models for the structure of outer-membrane proteins of *Escherichia-coli* derived from Raman-spectroscopy and prediction methods, *Journal of Molecular Biology 190*, 191-199.

Vogel, H., Nilsson, L., Rigler, R., Voges, K. P., and Jung, G. (1988) Structural fluctuations of a helical polypeptide traversing a lipid bilayer, *Proceedings of the National Academy of Sciences of the United States of America 85*, 5067-5071.

Yguerabi.J, Epstein, H. F., and Stryer, L. (1970) Segmental flexibility of an antibody molecule, *Journal of Molecular Biology 51*, 573-&.

Zakharian, E., and Reusch, R. N. (2005) Kinetics of folding of Escherichia coli OmpA from narrow to large pore conformation in a planar bilayer, *Biochemistry 44*, 6701-6707.